CYPRUS UNIVERSITY OF TECHNOLOGY

FACULTY OF ENGINEERING AND TECHNOLOGY

Master Thesis

THE RISK OF CORROSION IN STRUCTURES DUE TO CARBONATION USING GIS TOOLS

Nikolas Georgiou

Limassol 2015

CYPRUS UNIVERSITY OF TECHNOLOGY

FACULTY OF ENGINEERING AND TECHNOLOGY

DEPARTMENT OF CIVIL ENGINEERING AND GEOMATICS

THE RISK OF CORROSION IN STRUCTURES DUE TO CARBONATION USING GIS TOOLS

by

Nikolas Georgiou

Limassol 2015

APPROVAL FORM

Master thesis

The risk of corrosion due to carbonation in structures using GIS tools

Presented by

Nikolas Georgiou

Supervisor:

...……

Committee member:

……

Committee member:

……

Cyprus University of Technology

September, 2015

Copyrights

The adoption of the master thesis from the Department of Civil Engineering and Geomatics of Cyprus University of Technology does not necessarily imply acceptance of the authors views on behalf of the Department.

Σημειώνεται ότι η εν λόγω διπλωματική εργασία εντάσσεται μέσα στις ερευνητικές δραστηριότητες της Δρ. Έλια Α. Ταντελέ στο οποίο συμμετέχει η ερευνητική ομάδα infrastruc$_t$ure^2 του Τμήματος ΠΟΜΗΓΕ του ΤΕΠΑΚ.

I would like to thank everyone that supported me with the completion of my thesis. Also my professors for all they have taught me and their help. Especially i would like to thank my supervisor Dr. Elia Tantele for her support and help that contributed towards completing my thesis.

ΠΕΡΙΛΗΨΗ

Μέσα από τις εξελίξεις της τεχνολογίας του σήμερα η δυνατότητα συγκέντρωσης, επεξεργασίας και να διάδοσης πληροφοριών έχει γίνει πολύ πιο αποτελεσματική με τη χρήση εργαλείων όπως τα ΓΣΠ. Για τους πολιτικούς μηχανικούς οι πληροφορίες δεν είναι πάντα διαθέσιμες και αυτό οδηγεί σε δαπανηρό και χρονοβόρο πειραματισμό από την πλευρά τους, ώστε να είναι σε θέση να αποκτήσουν τις απαραίτητες πληροφορίες που αφορούν τα κτίρια. Η διάβρωσης του χάλυβα οπλισμού είναι ένα από τα πράγματα που χρειάζονται τέτοια πειράματα, προκειμένου να επιβεβαιωθεί κατά πόσο είναι υπαρκτή. Η μελέτη αυτή θα επικεντρωθεί ειδικότερα στην Κύπρο και πώς η διάβρωση του χάλυβα είναι ένα σημαντικό ζήτημα εδώ. Δίνεται μια περιγραφή της διαδικασίας διάβρωσης με έμφαση στην ενανθράκωση του σκυροδέματος αφού θεωρείται η πιο κοινή περίπτωση για τη συγκεκριμένη μελέτη. Η διάβρωση λόγω ιόντων χλωρίου επίσης αναφέρεται, δεδομένου ότι είναι συνήθως ο κύριος παράγοντας διάβρωσης. Η μελέτη λαμβάνει υπόψη της διάφορες μελέτες που αφορούν τους παράγοντες που επηρεάζουν τη διάβρωση σε σχέση με τον ρυθμό της διάβρωσης, ή άλλες πληροφορίες που είναι ζωτικής σημασίας για να κατανοήσουμε πώς επηρεάζεται η διάβρωση. Οι πληροφορίες που αποκτούνται χρησιμοποιούνται για να δημιουργηθεί ένα μαθηματικό μοντέλο για την πρόβλεψη του κινδύνου διάβρωσης. Στη συνέχεια εισάγεται η χρήση των ΓΣΠ σε συνδυασμό με το μαθηματικό μοντέλο που αναπτύχθηκε για να βρεθεί πού είναι πιο πιθανό να υπάρχουν προβλήματα διάβρωσης. Η μελέτη ολοκληρώνεται με μερικά συμπεράσματα σχετικά με τη χρήση των Γεωγραφικών Συστημάτων Πληροφοριών και πώς μπορούν να βοηθήσουν στο πρόβλημα του προσδιορισμού της διάβρωσης.

Λέξεις κλειδιά: διάβρωση, επικινδυνότητα διάβρωσης, μαθηματική μοντελοποίηση της διάβρωσης, ΓΣΠ

ABSTRACT

Through the technology advancements of this time the ability to gather, process and distribute information has become a great deal more efficient by using tools like GIS. For civil engineers information is something that is not always available and this leads to expensive and time consuming experimentation from their part in order to be able to gain the information necessary that concerns buildings. Steel reinforcement corrosion is one of the things that need such experiments in order to be confirmed. This study will focus specifically on Cyprus and how corrosion is an important issue here. A description of the process of corrosion is given with focus on the carbonation of the concrete since it is considered the most common process for this particular case study. Chloride ion corrosion is also mentioned since it's the leading factor of corrosion. The study takes into consideration various studies that relate factors that affect corrosion to the rate of corrosion, or other information that is critical to understand how corrosion is affected. The information gained is used to create a mathematical model to predict corrosion risk. The use of GIS is then introduced in conjunction with the mathematical model in order to find where it is most probable to come across corrosion problems. The study ends with a few conclusions about the use of GIS and how it can help the problem of identifying corrosion.

Keywords: corrosion, corrosion risk, mathematical modeling of corrosion, carbonation, GIS

TABLE OF CONTENTS

LIST OF TABLES

LIST OF FIGURES

NOTATIONS

RC:	Reinforced Concrete
NDT:	Non-Destructive Test
AASHTO:	American Association of State Highway and Transportation Officials
GIS:	Geographical Information System
SCE:	Saturated Calomel Electrode
CSE:	Copper Sulfate Electrode

INTRODUCTION

Corrosion of steel reinforcement in Cyprus is very apparent due to the fact that reinforced concrete is the most popular building material. In the recent years corrosion is observed on a lot of the buildings making failure of a lot of constructions a thing to worry about. This paper will be focusing on the area of Limassol and specifically the areas that are more affected by carbonation rather than chloride ions. The biggest problem when facing corrosion is identifying where it is since it is not always easy to see only by visually inspecting the state of a structure. Most of the time we have to wait until the damage to the reinforcement becomes big enough to be noticeable, and then conduct experiments and lab tests to determine exactly how bad the damage is. In the recent years reliability methods are used in order to predict which areas are the most susceptible to corrosion in an attempt to prevent various dangerous situations like collapsing of buildings from happening. In this paper these reliability methods are used while implementing them in programs like GIS tools in order to achieve a reliability assessment of structures over a large area in Limassol. This assessment is gained from the creation of maps that relate various data that affect corrosion with the use of mathematical modeling to the risk of corrosion occurring. The end result gives engineers probabilistic knowledge concerning corrosion, in order to help them at designing, monitoring or taking the correct decisions concerning structures.

1 Corrosion

1.1 Corrosion History

The process of corrosion can be identified as a major drawback for all products created by metallic materials since a long time ago. For civil engineers though the scale and effect of corrosion is substantially greater in their work when compared to others since the scale of the products designed by civil engineers is many times bigger. Construction steel is the basic material civil engineers use in order to give a member of the structures they design enough tensile strength to carry the loads required by the design. Whether the product of the design is a house, skyscraper, bridge or any other structure civil engineers design the effect of corrosion worldwide can be measured in billions of euro that have to be spend in order to replace corroded parts from a structure, repair damages to structures that were caused by corrosion or simply by taking into account the monetary loss from losing a structure due to corrosion. Corrosion has been categorized into two different phenomena's distinguished by the way the metallic material corrodes. The first one is uniform corrosion where corrosion occurs uniformly on the whole surface of the metal and rust forms on the surface resulting in the material becoming thinner. The second form of corrosion is localized corrosion where corrosion occurs on a specific spot of the metal, but the rate of corrosion is very fast resulting in great loss of material locally. Localized corrosion is usually observed on materials that are seen as corrosion resistant such as aluminum alloys or stainless steel after suffering from fatigue.

1.2 Corrosion as an electrochemical process

The nature of corrosion is electrochemical. The electrochemical process can be explained as the formation of a double electrical layer where the surface of a metal comes in contact with a liquid. The reason this layer is formed stems from the interaction between the metal and liquid which is considered the electrolyte of this interaction, where an anode is generated and sustained by the continuation of metallic or hydrated ions constantly passing through the liquid. This results in the rusting of the metal as the metal ions are constantly leaving the metal to enter the liquid. The chemical equation describing the process of corrosion for iron is (Pietro 2013):

$$Fe(s) \rightarrow Fe^{++} + 2e^{-}$$

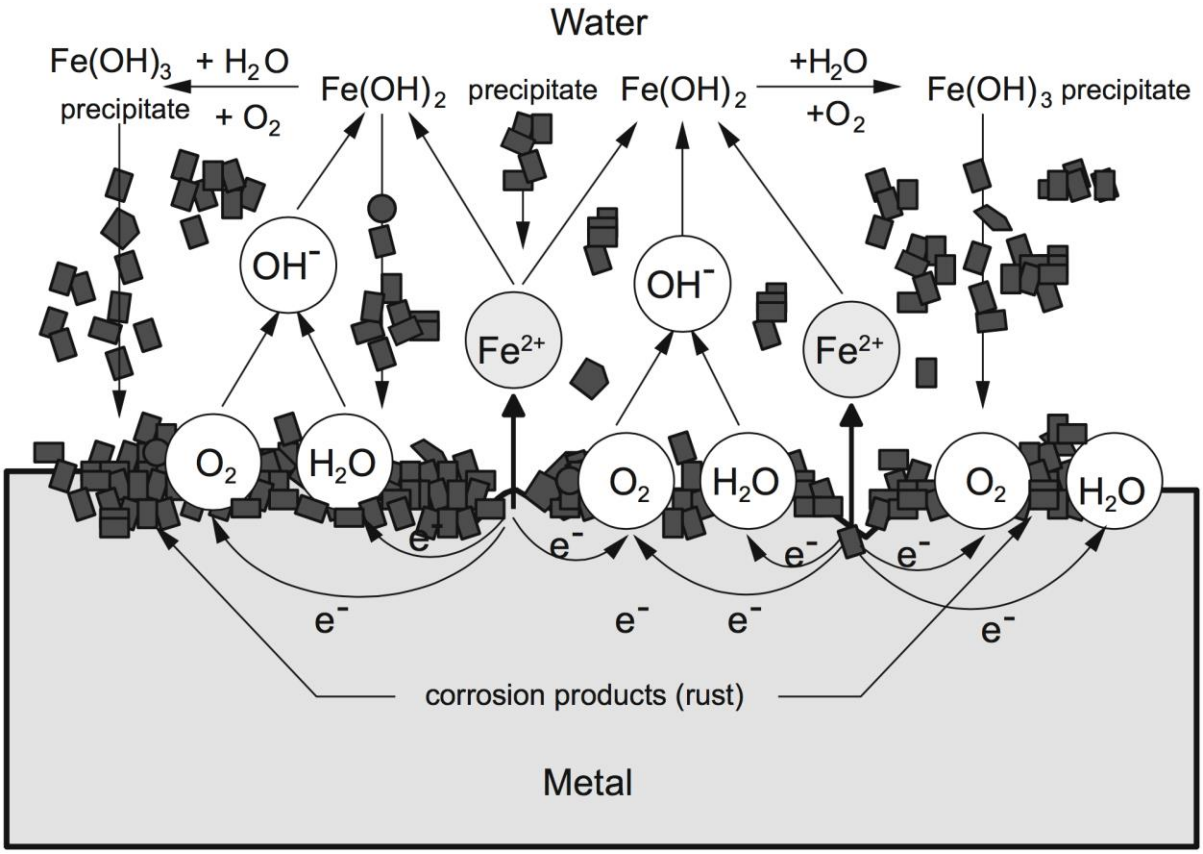

Figure 1: Schematic view of iron corrosion with rust production (Pietro 2013)

Corrosion is the deterioration of steel reinforcement due to electrochemical reactions, which cause the steel to rust and change form (Figure 1), until in the most extreme of cases, there is no steel remaining inside the concrete. As is expected this results in dangerously low strength concrete with many problems that may eventually cause failure of the construction. There are two main reasons that corrosion occurs. The first reason is carbonation of the concrete and the second one is chloride ions that exist in the atmosphere around the concrete. For carbonation to occur, large amounts of CO_2 need to be present close to the reinforced concrete. We can safely assume that most CO_2 exposure will be seen close to main roadways and industrial zones since that is where most CO_2 generating functions are found. Chloride ions are found where there is saltwater or salt used for ice melting. In this study the inner area of Limassol is presumed to be of highest importance and therefore it is the area that this study will be the most concerned with. Since the area of concern is the inner part of Limassol where seawater is not present, we can safely assume that carbonation is the main corrosion catalyst instead of chloride ions.

Corrosion has been related to the cracking of the concrete in many cases as seen in (Figure 2). There are really not many conclusive studies made that have made it apparent whether that relation is existent but it is true that cracking in concrete results in faster initiation of corrosion and that some studies claim that by measuring the width of the crack you can also measure the risk of corrosion. A study though (Hansen et al. 2015) supports that the cracking's effect on corrosion is minimal when compared to other factors that influence corrosion and it is debatable whether it should be taken into account.

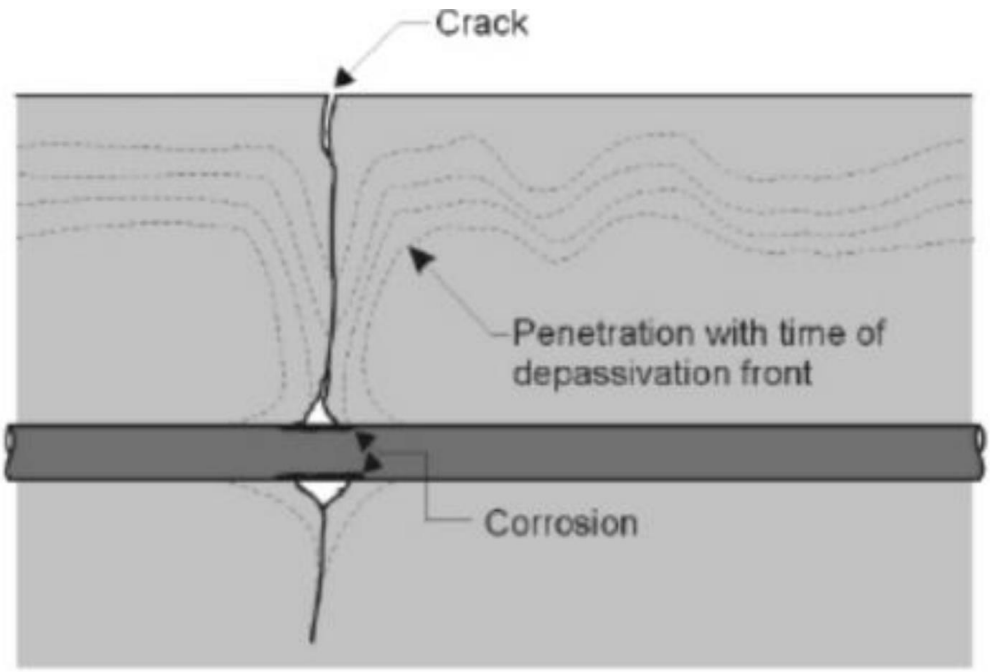

Figure 2: Illustration of the penetration of the depassivation front (Bertolini, Luca, Elsener, Bernhard, Pedeferri, Pietro, Redaelli, Elena, Polder 2013)

For the prevention or diminishing of the corrosion process can be enhanced by the use of inhibitors in the concrete. However as noted in a study (Kondratova et al. 2003) it is extremely important that the concrete does not crack too much since that makes the protection from the inhibitors obsolete, and that is really hard to achieve since the cracking of concrete is quite usually observed during its service time.

Another way to monitor and possibly prevent corrosion in structures is with the use of monitoring systems that are installed inside the RC structure. This sort of measure is especially recommended for constructions regarding infrastructure where the corrosion effect can have catastrophic subsequences if left unnoticed. The systems usually have a variety of different sensors embedded inside the concrete of the structure that continuously take measurements as shown in (Figure 3).

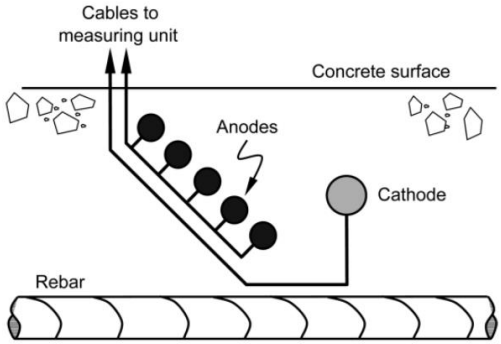

Figure 3: Ladder arrangement for monitoring macrocell current(McCarter and Vennesland 2004)

1.2.1 Carbonation

Carbonation is the process of Carbon Dioxide reacting with Hydroxides in order to form Carbonates. This of course is more apparent in areas with high Carbon Dioxide concentration. The Calcium Hydroxide in concrete usually reacts with the Carbon dioxide in the atmosphere that permeates the concrete, in order to form Calcium Carbonate. This results in a lower pH of the concrete that in turn enhances the corrosion process of steel reinforcement.

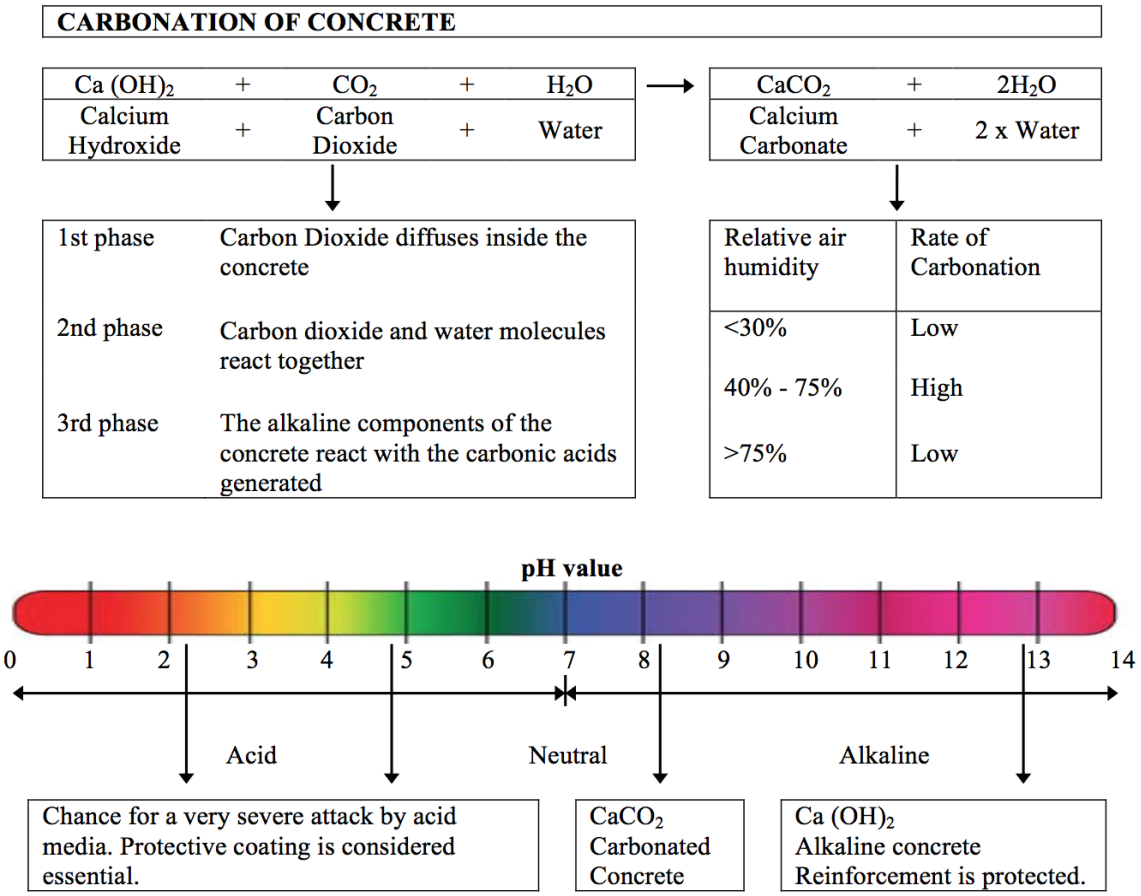

Figure 4: The carbonation process of concrete ("Kamta Corporation - Goa , INDIA" n.d.)

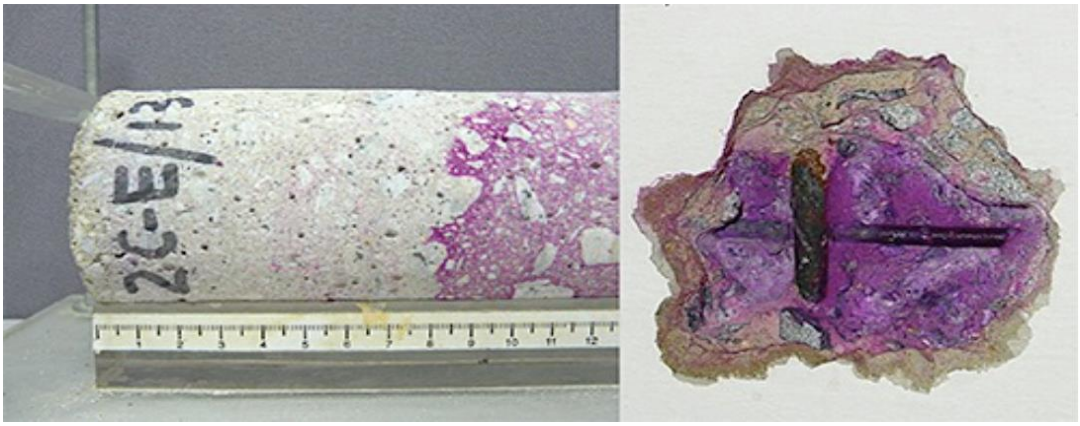

Figure 5: Carbonated concrete sample ("AL Technologies - Building Technology" n.d.)

Carbonation is a process that slowly progresses with time (Figure 4). A study (Ph. Turcry, L. Oksri-Nelfia, A. Younsi 2014) has shown in 14-day accelerated carbonation test that the carbonation process is practically nonexistent for the first half day. For the rest of the day though the carbonation increases at an extreme rate. The remaining days show that carbonation is linear to the square root of the time since it remains so until the end of the test. To check the process of carbonation in concrete it is common to use phenolphthalein, which makes the carbonated area more obvious (Figure 3).

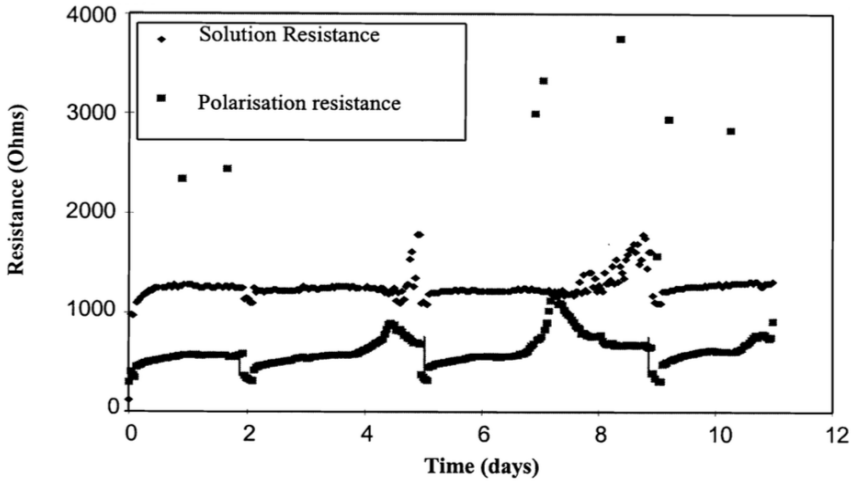

Figure 6: Effect of extended drying period on solution resistance and polarization resistance for carbonated specimens (Millard et al. 2001)

In another study (Keun-Hyeok Yang, Eun-A Seo 2014) it is shown that the carbonation process is influenced by the humidity, supplementary materials used in the concrete and the type of finishing material used. The humidity is the most important factor when there is corrosion since it is the material that is used as an electrolyte in order for the electrochemical process of corrosion to start(Saha 2013). The effect of humidity and lack of humidity can also be seen in (Figure 5). Some supplementary materials that are used in

concrete can slow down the corrosion process by disrupting the electrochemical reaction up to a certain point, however it is not possible to completely stop corrosion. The most obvious method of protecting the concrete is by protecting it from the outer atmosphere by applying special finishing materials that won't allow carbon dioxide or moisture to reach the concrete. Even with that there is no perfect solution currently to the problem of corrosion, therefore finding and repairing the damage caused by corrosion in time is the most important thing to prevent future structure deterioration. A different study (SOHAIL 2013) claims that the main reason that carbonation is so easy to happen in reinforced concrete is because the pores inside it are connected at a great degree. It is noted that this is connected to the way concrete is structured. This makes it easy for the carbon dioxide to move inside the reinforced concrete and consequently initiate the carbonation that will lead to the fall of the pH until the reinforcement steel begins corroding.

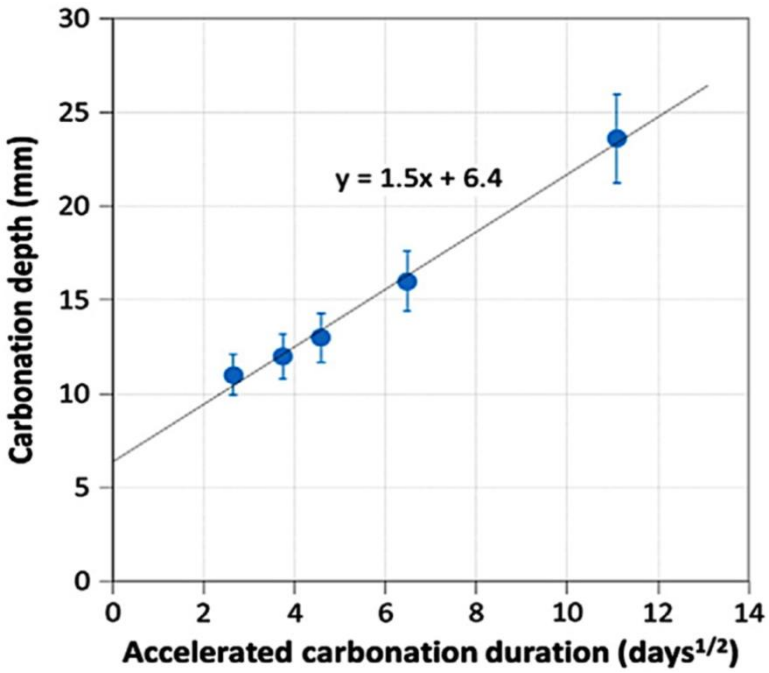

Figure 7: Depth of the carbonation in concrete in relation to time according to the French Standards protocol (Ph. Turcry, L. Oksri-Nelfia, A. Younsi 2014)

1.2.2 Chloride ions

Other than the corrosion factor that is mainly discussed in this paper that is carbonation, the chloride ions that are the other corrosion factor are also extremely important and in many cases more apparent than carbonation. The cases where corrosion from chlorides is prevalent are usually found near coast lines, since seawater is the main source of chloride

ions. The penetration of chloride ions inside the concrete of RC structures has a specific rate depending on various factors such as the concrete cover as seen in (Figure 5). Another factor that is mentioned in studies as something that resists the diffusion of chlorides in the concrete and in turn also the rate of corrosion are sulfate ions, since they fill the pores within the concrete (Liu et al. 2012).

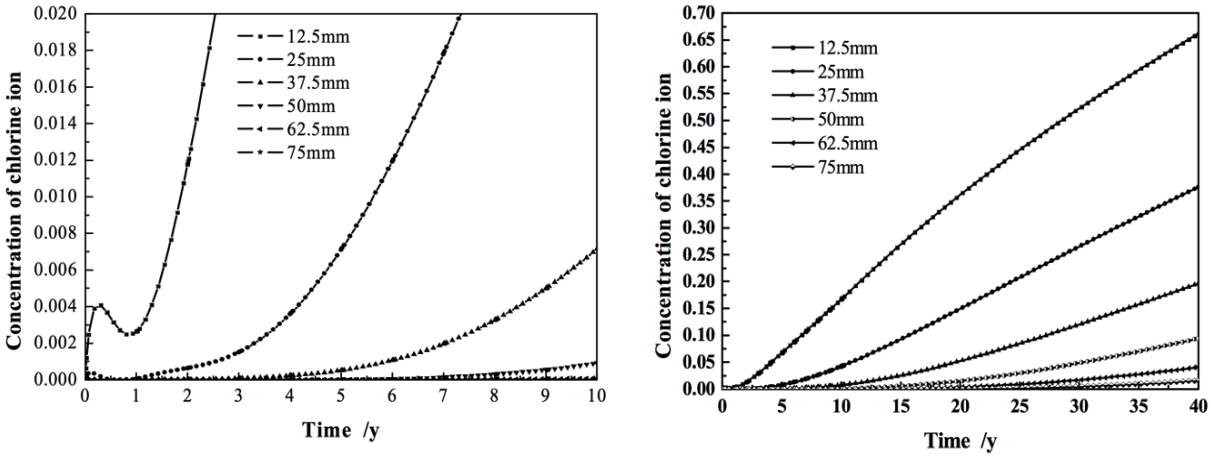

Figure 8: Chloride ion concentration (Song et al. 2012)

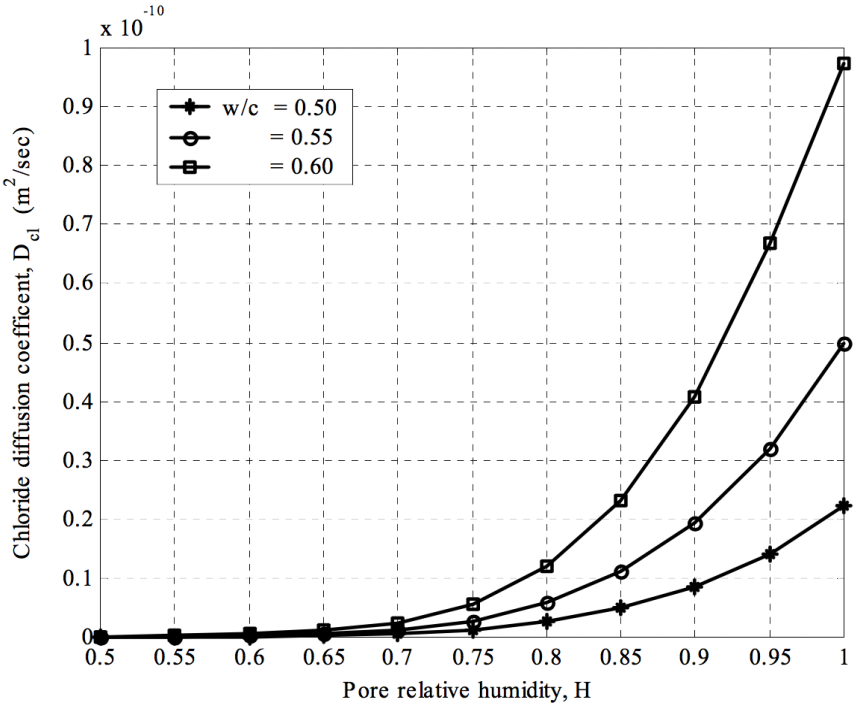

Figure 9: Effect of water-cement ratio on chloride diffusion (Ababneh et al. 2003)

For corrosion to initiate though there are other factors that have to be present. The factors that will contribute or affect the initiation of the corrosion process are the pH of the concrete, the humidity of the environment, the temperature, the electrical resistivity of the concrete and oxygen. The mixture of the concrete is also something that will greatly affect the rate of corrosion since the addition of admixtures in the concrete or the water-cement ratio influence the physical aspects of the concrete as shown in (Figure 6). In general chloride corrosion is considered many times faster than carbonation corrosion of steel, however there are studies that claim the opposite for certain circumstances (Chen et al. 2012), therefore that cannot be considered as a fact but more as a general observation.

The effects of corrosion due to chloride ions are the same as the effects of corrosion due to carbonation. In other words the problem in both cases is the deterioration of the construction steel within the reinforced concrete, which in turn leads to a reduced tensile strength of the member and danger of collapse for the structure.

2 Corrosion measurements

For the identification and quantification of corrosion civil engineers use tools or experiments that can help them measure the values they need. The methods involving measurements in RC structures can be divided in two main groups. The first group contains the Destructive Tests and the second one contains the Non Destructive Tests (NDT).

2.1 Open Circuit Potential (OCP)

In this test the corrosion potential of construction steel is measured in relation to a standard reference electrode like SCE or CSE. This test belongs to the NDT group of tests and is considered a very useful way of finding when corrosion will occur if the rebar is exposed to the environment (Song and Saraswathy 2007)

2.2 Surface Potential (SP)

The surface potential test (SP) also belongs to the group of NDT. This test is similar to the OCP test but it allows for the measurement of the condition of the rebar while it is inside the concrete which is more useful in some situations. The technique entails having an electrode fixed on the structure while having another electrode moving along the structure and measuring the potential of the moving electrode compared to that of the fixed one with a high impedance voltmeter (Song and Saraswathy 2007).

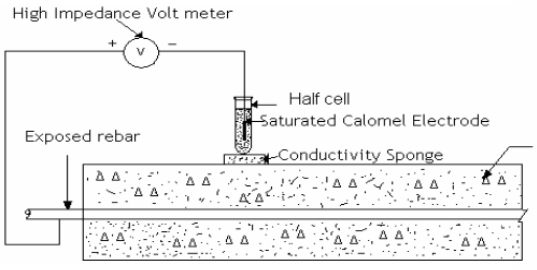

Figure 11: Schematic representation of Open circuit potential (OCP) measurement (Song and Saraswathy 2007)

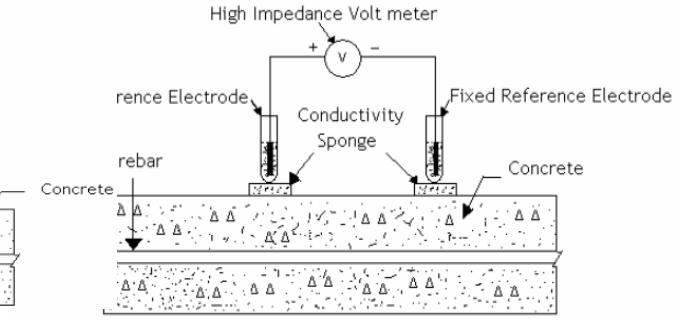

Figure 10: Schematic representation of surface potential (SP) measurements (Song and Saraswathy 2007)

2.3 Linear Polarization Resistance (LPR)

The linear polarization resistance test belongs to the NDT of corrosion measurements, however a certain extent of the damage on the concrete is needed, but is kept only to a minimum since it only requires enough penetration into the concrete to allow for an electrical connection to be made to the rebar. The information gathered from this method though is much more detailed when compared to the previous methods. The measurements taken by the use of this method are affected by temperature and humidity, a fact that you have to keep in mind (Song and Saraswathy 2007).

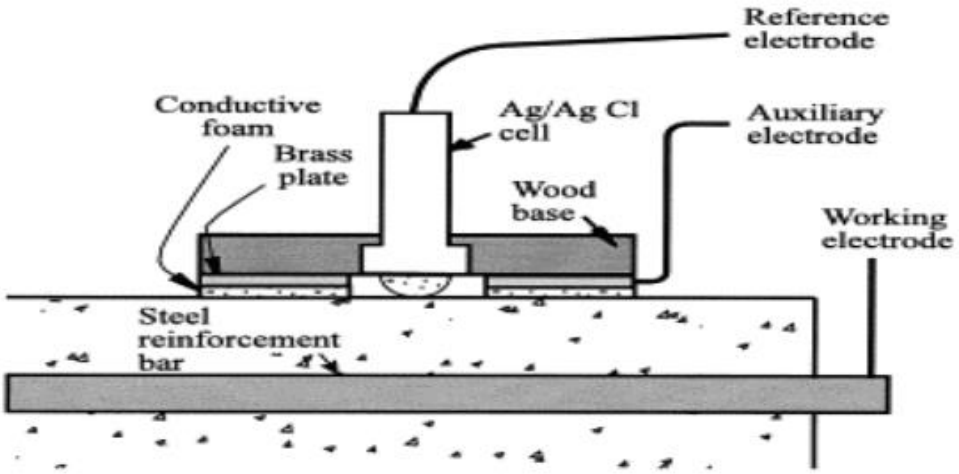

Figure 12: Linear polarization resistance measurement (Song and Saraswathy 2007)

There are also other NDT like Harmonic Analysis, Noise Analysis, Radiography measurement, Concrete Resistivity, Visual inspections and others.

2.4 NordTest (NT) method

This method belongs to the destructive tests where samples from drilling are needed to conduct the tests. This test determines the chloride migration coefficient which is used to determine the resistance of the concrete sample to chloride penetration. This test is broadly used to measure the corrosion due to chlorides in structures. The arrangement of the migration set-up is seen in (Figure 13: Arrangement of the migration set-up **(NORDTEST 1999)**).

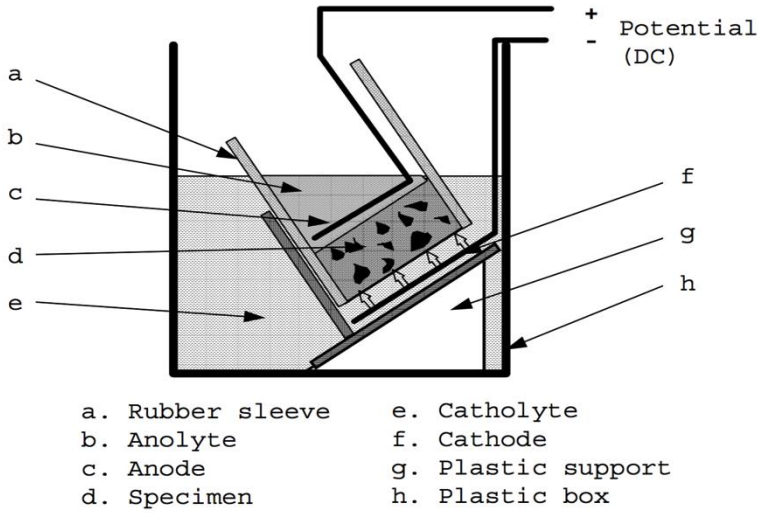

Figure 13: Arrangement of the migration set-up (NORDTEST 1999)

2.5 Mesaurement of concrete carbonation depth

This test belongs to the destructive methods of testing since it requires samples from drilling of the concrete. The samples are then broken in half and the chemical phenolphthalein is sprayed on the broken parts of the samples. The parts of the concrete that change color are those that still have a high pH value. The parts though that don't change color are those where the pH value has decreased and if they reach the steel reinforcement, then the corrosion will initiate. The test measures the width of penetration into the concrete from the point where the specimen does not change color until the surface of the concrete (Naik and Science 2004).

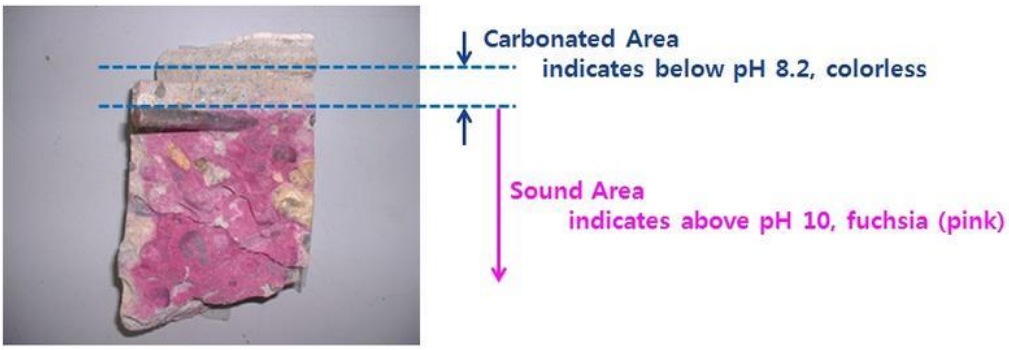

Figure 14: Test sample ("Carbonation of Concrete" n.d.)

3 Developing the Mathematical Model

3.1 Correlation between data acquired from studies and corrosion

For the purpose of correlating a variety of data and corrosion, a number of different researches are taken into account while trying to surmise and compress everything in order to create a mathematical model that can give us a rough estimate of the risk of corrosion in an area. The mathematical model generated is only a primary effort at creating a model to use with GIS tools in order to create corrosion risk maps, and should not be considered as accurate or a representation of reality. For the model to be used extensively in real situations further refinement, experimentation and testing is required.

3.1.1 Estimation of steel corrosion using half-cell potential method

Data from the use of half-cell potential method is used to estimate corrosion rate in a paper by Zhu and Dai (Zhu and Dai 2012). In this paper they used the linear polarization method experiment to regress the correlation between the corrosion current and the corrosion potential. It was considered appropriate to use the regression equation because the results found from using the half-cell potential method and the linear polarization resistance method were deemed to be close enough. The paper concludes that the relationship corrosion current and corrosion potential is exponentially regressive and that indeed the results from half-cell potential method and linear polarization resistance method are fairly close.

No.	C.T.	L.P.R		H.P.		No.	C.T.	L.P.R		H.P.	
	mm	C.C $\mu A/cm^2$	C.P mV	C.P mV	C.C.C $\mu A/cm^2$		mm	C.C $\mu A/cm^2$	C.P mV	C.P mV	C.C.C $\mu A/cm^2$
A1-1	10	0.801	-512	-500	0.343	A4-3	10	0.262	-563	-552	0.512
	45	0.438	-493	-488	0.312		45	0.963	-553	-543	0.477
A1-2	10	1.371	-539	-511	0.373	A8-1	10	0.200	-356	-323	0.088
	45	0.311	-304	-310	0.079		45	0.196	-370	-326	0.090
A1-3	10	2.480	-525	-488	0.312	A8-2	10	0.078	-378	-361	0.117
	45	0.942	-505	-466	0.265		45	0.178	-420	-350	0.108
A5-1	10	0.151	-188	-192	0.032	A8-3	10	0.363	-350	-332	0.094
	45	0.221	-205	-201	0.034		45	0.333	-367	-323	0.088
A5-2	10	0.176	-292	-343	0.103	A7-1	10	1.689	-561	-523	0.410
	45	0.159	-287	-323	0.088		45	1.282	-537	-509	0.368
A5-3	10	0.068	-175	-201	0.034	A7-2	10	0.542	-549	-537	0.456
	45	0.080	-200	-208	0.036		45	1.388	-544	-514	0.383
A4-1	10	0.774	-587	-579	0.631	A7-3	10	1.316	-538	-536	0.451
	45	0.763	-588	-569	0.583		45	1.416	-523	-503	0.352
A4-2	10	0.704	-558	-556	0.526						
	45	0.289	-558	-550	0.503						

Table 1: Test results (Zhu and Dai 2012)

where: C.T. = Cover Thickness

L.P.R. = Linear Polarization Resistance method

H.P. = Half-cell Potential method

C.C. = Corrosion Current

C.E. = Corrosion Potential

C.C.C. = Calculated Corrosion Current

The results from the research done here can give as a better understanding of how corrosion is affected by the mixture of the concrete and the cover of the construction steel that is contained within the concrete.

3.1.2 Comparison of different algorithms in their accuracy to measure construction steel corrosion

In a study by Pingjie Cheng (Cheng 2012) the accuracy of a number of different algorithms at estimating construction steel corrosion is assessed and compared to real results. Pingjie Cheng supports that the support vector machine algorithm is the most accurate and explains the function and application of said algorithm. The study concludes that predicting how extensive steel corrosion is in a structure is a nonlinear problem, and therefore using linear empirical formulas will result in inaccurate results. Also Pingjie Cheng notes that the support vector machine algorithm is the most optimum when the sample size is very small since it requires very little training and produces sufficiently accurate results. The nonlinear regression function for the support vector machine algorithm is:

$$f(x) = \sum_{i=1}^{i} (a_i - a_i^*) K(x_i, x) + b \qquad (1)$$

The function depicted in the support vector machine algorithm can be used or taken into account when trying to construct the mathematical model concerning the probability of corrosion in an area.

3.1.3 Investigating Macrocells to estimate corrosion rate

There is a study concerning a new method of estimating the rate of construction steel corrosion (Raupach and Gulikers 2015) by a method based on investigating macrocells. Raupack and Gulikers in this study predict the macrocell action in reinforced concrete by using equivalent electrical circuit models to conduct a numerical simulation of structural steel

corrosion. The simulation was conducted for a well-defined geometry with plan parallel and coplanar arrangement of steel for both actively corroding and passive variations. For the case of the plan parallel arrangement the situation studied was two-dimensional and concerned the conjoint action of microcells and macrocells. For the case of the coplanar arrangement they used a transmission line model. The equation used to express macrocell action between the two variations of steel is:

$$I_{gal} = \frac{U_C - U_A}{R_{\rho,C} + R_{con} + R_{\rho,A}} \tag{2}$$

where: I_{gal} = Galvanic current

$U_C - U_A$ = Potential difference between passive (Cathodic) and corroding (Anodic) areas

R_ρ = Resistance against polarization

R_{con} = Electrolyte concrete resistance

For the expression of microcell action the equation used is:

$$i = i_{corr}\left[exp\left(\frac{ln(10)\cdot \Delta U}{b_a}\right) - exp\left(\frac{-ln(10)\cdot \Delta U}{b_c}\right)\right] \tag{3}$$

where: i = Current density

i_{corr} = Corrosion current density

$\Delta U = U_C - U_A$

b_a = Anodic Tafel slope

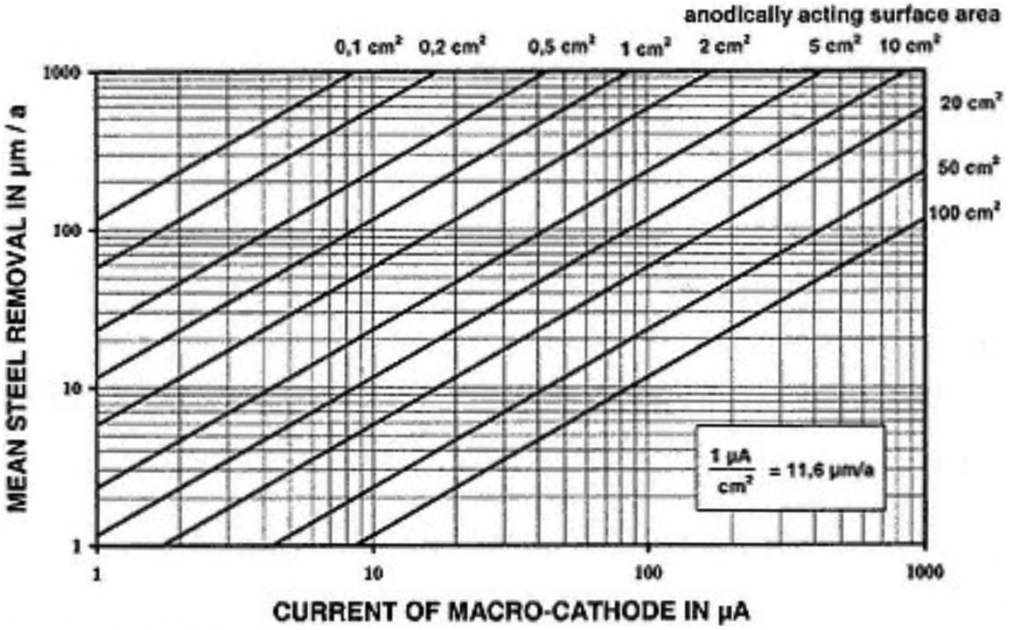

Figure 15: Steel removal in relation to current of macro-cathode (Cheng 2012)

The study concludes that macrocell action plays an important role in the corrosion of construction steel. Cheng says that it is possible to predict the electrochemical interactions happening inside the steel reinforcement by the use of numerical analysis. The study also notes the faults of simplified models since the correct prediction of macrocell current flow requires all factors of the driving voltage, concrete electrolyte resistivity and polarization behavior of the passive steel. The final conclusion is that the rate of corrosion is at its peak when the exposure area of the macro-cathodes is big when compared to the corroding area.

It is evident in this study that the steel and electrolyte as well as the conditions of the concrete and the environment greatly influence the rate of corrosion. The models used to depict this corrosion rate can be analyzed and incorporated in the mathematical model that this paper is trying to suggest.

3.1.4 The effect of temperature

The temperature is another factor that influences the rate of corrosion in structures as noted in a study about the effect of temperature on the corrosion of steel in concrete (Pour-Ghaz et al. 2009). The effect was investigated by using simulated polarization resistance experiments. For the purpose of the simulation for a wide range of possible anode/cathode distributions of construction steel, the numerical solution of the Laplace equation was used in a way that created independent correlations between temperature, corrosion rate, kinetic parameters, limiting current density and concrete resistivity. From the experiment results Ghaz et al. managed to develop a prediction model for the corrosion rate of steel reinforcement in structures. The end result of the experiments was the equation:

$$i_{corr} = a_3 \frac{1}{\rho^{c1}} + a_{14} \frac{(T i_L)^{b14}}{\rho^{c1}} + a_{15} \frac{T^{b15} b_{15}^{i_L^{c15}}}{\rho^{c1}} + a_{124} \frac{T d^{b'_{124}} i_L^{b''_{124}}}{\rho^{c1}} + a \qquad (4)$$

where: i_{corr} = Rate of corrosion

a, b, c = Coefficients of the equation

ρ = Resistivity

T = Effect of kinetic parameters

d = Cover thickness

i_L = Limiting current density

The equation was then used to create a new set of equations for average and maximum current density:

$$\begin{Bmatrix} i_{corr,ave} \\ i_{corr,max} \end{Bmatrix} = \frac{1}{\tau\rho^{\gamma}}\left(\eta T d^{\kappa} i_L^{\lambda} + \mu T v^{i_L^{\omega}} + \theta (T i_L)^{\theta} + \chi\rho^{\gamma} + \zeta\right) \quad (5)$$

where: $i_{corr,ave}$ = Average current density

$i_{corr,max}$ = Maximum current density

T = Effect of kinetic parameters

d = Cover thickness

i_L = Limiting current density

τ, ρ, γ, η, κ, λ, μ, ν, ω, θ, χ, ζ = Coefficients of the equation

$i_{corr,ave}$		$i_{corr,max}$	
Constant	Value	Constant	Value
τ	$1.181102362 \times 10^{-3}$	τ	1
η	$1.414736274 \times 10^{-5}$	η	0.32006292
ζ	−0.00121155206	ζ	−53.1228606
κ	0.0847693074	κ	0.00550263686
λ	0.130025167	λ	0.120663606
γ	0.800505851	γ	0.787449933
μ	$1.23199829 \times 10^{-11}$	μ	$-3.73825172 \times 10^{-7}$
θ	−0.000102886027	θ	47.2478753
ϑ	0.475258097	ϑ	0.00712334564
χ	$5.03368481 \times 10^{-7}$	χ	0.003482058
ν	90487	ν	784679.23
ϖ	0.0721605536	ϖ	0.0102616314

Table 2: Constants of the equation (Pour-Ghaz et al. 2009)

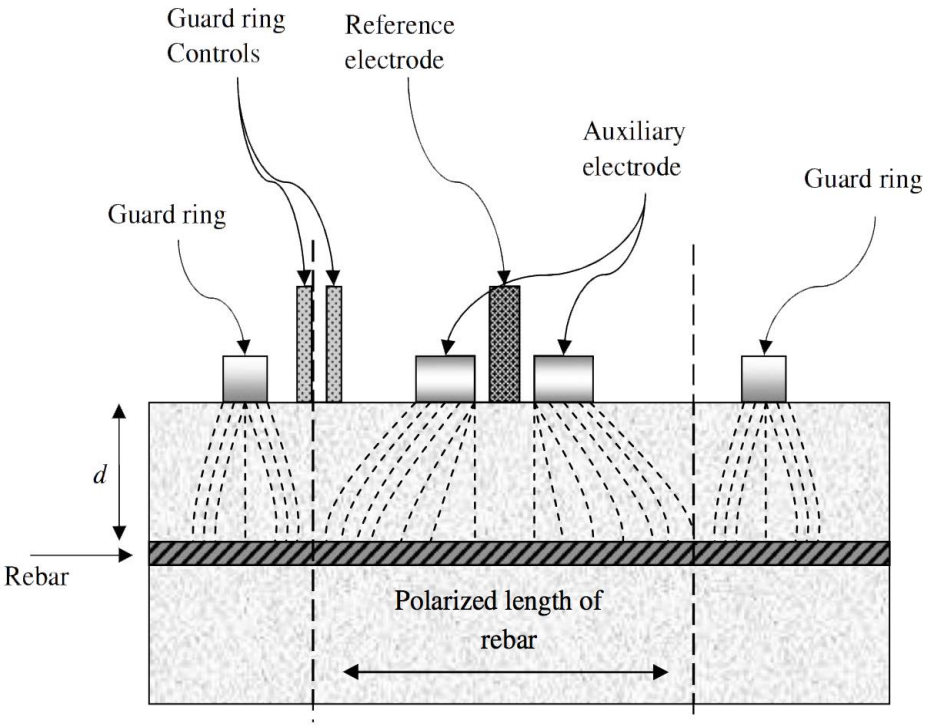

Figure 16: Schematic of polarized resistance test setup (Pour-Ghaz et al. 2009)

The conclusions and observations from the simulations are that the relation between corrosion rate and temperature is linear if you consider that the temperature only affects the kinetic parameters. For the experiments the range of temperature tested was from 283-323 K (≈10-50 C°). For this range of temperature the changes to corrosion rate observed where up to 20%. Another observation is that the effect of limiting current density on corrosion rate diminishes when the concrete resistivity is high. When all parameters but resistivity are constant it is shown that resistivity has the most influence on corrosion rate. For the case of all parameters being constant except for limiting current density an increase of about 30% for the predetermined range of temperatures. A bizarre observation is the increasing rate of corrosion as the concrete cover thickness increases. It is noted however that the increase in corrosion rate due to the cover thickness is limited by how high concrete resistivity is as it is observed that high concrete resistivity makes this effect less prevalent. A final observation by Ghaz et al. is that the rate of corrosion increases rapidly with the increase of limiting current density, with that rapid increase slowing down at higher values until it becomes stable.

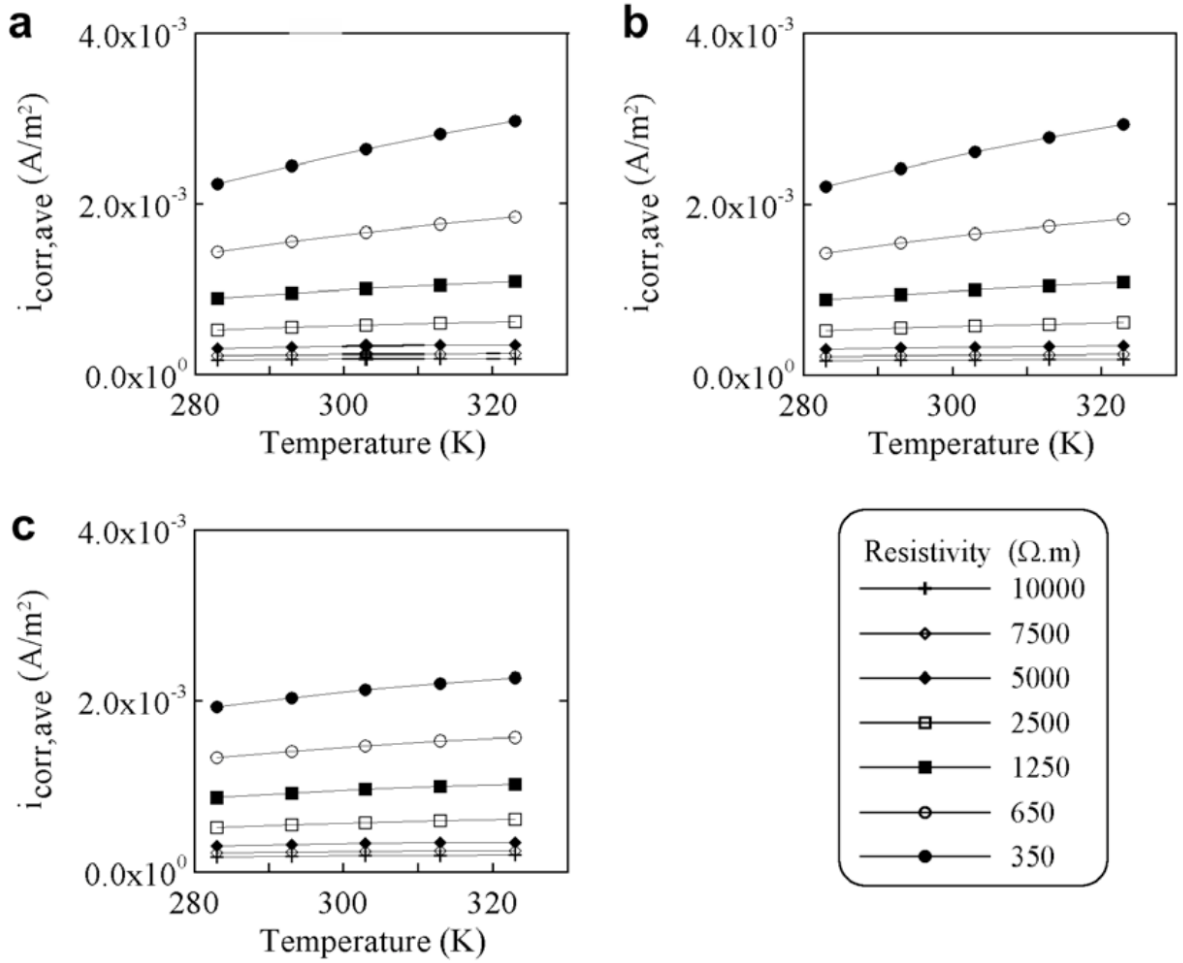

Figure 17: Variation of corrosion rate with temperature (affecting only kinetic parameters) for different values of concrete resistivity (60 mm cover thickness): (a) i_L = 0.2 A/m^2, (b) i_L = 0.05 A/m^2, (c) i_L = 0.005 A/m^2. (Pour-Ghaz et al. 2009)

The research done in this study can provide us with a very clear image of how the temperature influences corrosion rate of construction steel in structures. The report given is very detailed and the results can be used when trying to unify all information about corrosion risk in a single equation.

3.1.5 Prediction of time from corrosion initiation to cracking

Another paper from El Maaddaway and Soudki (El Maaddawy and Soudki 2007) claims that the key to finding out what the service life of a corroded RC structure is the prediction of time to corrosion cracking. The relation between steel mass loss and the internal radial pressure that the corrosion products cause is represented by a model. The model for the concrete around the construction steel that has initiated corrosion is a thick-walled cylinder with a wall thickness equal to the thinnest concrete cover, with the assumption that when the tensile stresses in the circumferential direction surpass the concrete tensile strength cracks will form on the concrete ring. Then the relation between internal radial pressure and steel mass loss is determined, and the time from corrosion initiation to corrosion cracking is calculated using Faraday's law. El Maaddaway and Soudki authenticate their model by comparing it to experimental data that was published in other papers. The equation used to determine the time needed for corrosion cracking to occur since the corrosion initiates is:

$$T_{cr} = \left[\frac{7117.5(D + 2\delta_0)(1 + v + \psi)}{iE_{ef}}\right]\left[\frac{2Cf_{ct}}{D} + \frac{2\delta_0 E_{ef}}{(1 + v + \psi)(D + 2\delta_0)}\right] \qquad (6)$$

where: T_{cr} = Time from corrosion initiation to corrosion cracking

D = Diameter of the steel reinforcing bar

δ_0 = Thickness of porous zone

v = Poisson's ratio

ψ = Factor dependent on D, C and δ_0

i = Current density

E_{ef} = Effective elastic modulus of concrete

f_{ct} = Tensile strength of concrete

The authors of this study conclude that the model developed is satisfactory and the comparison with the experimental results from other studies authenticates its validity.

Therefore it can be assumed that this model can contribute to the model developed in this paper.

3.1.6 Reliability of reinforced concrete girders

A paper concerning the design of reinforced concrete bridge girders (Frangopol et al. 1997) through reliability methods that take into account the corrosion of construction steel. The approach in this particular paper is based on the American Association of State Highway and Transportation Officials (AASHTO) standards and data concerning corrosion of steel in concrete. The study investigates the effect of corrosion on moment and shear reliabilities and suggests a design based on reliability and minimization of total material cost while taking into account the effect of corrosion. This design is shown in different examples but the authors note that it can be improved upon by taking into account the minimization of expected lifetime cost and the cost of failure consequences. The reliability based design is expressed through the equation:

$$C_T = \frac{3}{4}\left(\frac{C_s Y_3}{144}\right) X_1 + \left(\frac{C_s X_{19} X_6}{1728}\right)(X_3 + X_5 - a + 0.5X_4) \quad (7)$$

where: C_T = Total cost

C_s = Unit cost of steel per 0.028 m^3

C_c = Unit of cost concrete per 0.0028 m^3

a = Distance from the bottom fiber to the centroid of reinforcement

X, Y = Variables defined in table

which is subject to the following constraints:

$$\beta_1(t) = \beta_M(t) \geq \beta_1^*;\ \beta_2(t) = \beta_{S1}(t) \geq \beta_2^*;\ \beta_3(t) = \beta_{S2}(t) \geq \beta_3^* \quad (8,9,10)$$

$$\beta_4(t) = \beta_{S3}(t) \geq \beta_4^*;\ g_3 = X_{12} - 0.75X_{13} \leq 0;\ g_4 = X_{21} - X_{12} \leq 0 \quad (11,12,13)$$

$$g_{5a} = X_7 - X_{20} \leq 0;\ g_{5b} = X_8 - X_{20} \leq 0;\ g_{5c} = X_9 - X_{20} \leq 0 \quad (14,15,16)$$

$$g_6 = X_{18} - 4X_{15} \leq 0;\ g_7 = 0.5X_4 - X_3 \leq 0;\ g_8 = X_2 - 4X_4 \leq 0 \quad (17,18,19)$$

$$g_9 = X_4 - X_2 \leq 0;\ g_{10} = -X_i \leq 0, (i = 1,2,\ldots,21) \quad (20,21)$$

where: β = Allowable reliability indices

β_M = Reliability index with respect to bending

β_S = Reliability indices with respect to shear

Notation (1)	Variable (2)	Units (3)
X_1	Area of the tension steel reinforcement, A_s	6.45 sq cm (1 sq in.)
X_2	Width of flange, b	2.54 cm (1 in.)
X_3	Thickness of flange, h_f	2.54 cm (1 in.)
X_4	Width of web, b_w	2.54 cm (1 in.)
X_5	Height of web	2.54 cm (1 in.)
X_6	Area of the shear reinforcement	6.45 sq cm (1 sq in.)
X_7	Spacing of shear reinforcement in interval 1	2.54 cm (1 in.)
X_8	Spacing of shear reinforcement in interval 2	2.54 cm (1 in.)
X_9	Spacing of shear reinforcement in interval 3	2.54 cm (1 in.)
X_{10}	Depth of equivalent rectangular stress block, a	2.54 cm (1 in.)
X_{11}	Nominal flexural strength of T beam	16.32 kN/m (1 kip/in.)
X_{12}	Reinforcement ratio, ρ	—
X_{13}	Balanced reinforcement ratio, ρ_b	—
X_{14}	Equivalent flange reinforcement	6.45 sq cm (1 sq in.)
X_{15}	Shear strength provided by concrete	4.45 kN (1 kip)
X_{16}	Shear strength provided by steel in interval 1	4.45 kN (1 kip)
X_{17}	Shear strength provided by steel in interval 2	4.45 kN (1 kip)
X_{18}	Shear strength provided by steel in interval 3	4.45 kN (1 kip)
X_{19}	Total number of stirrups required	—
X_{20}	Maximum shear reinforcement spacing	2.54 cm (1 in.)
X_{21}	Minimum bending reinforcement ratio	—
Y_1	Depth of slab	2.54 cm (1 in.)
Y_2	Center-to-center distance between girders	30.5 cm (1 ft)
Y_3	Girder span length	30.5 cm (1 ft)
Y_4	Specified yield strength of reinforcement, f_y	6.89 MPa (1 ksi)
Y_5	Specified compressive strength of concrete f'_c	6.89 MPa (1 ksi)
Y_6	Dead load excluding girder weight	14.59 kN/m (1 kip/ft)
Y_7	Maximum live load moment including impact	1.36 kN/m (1 kip/ft)
Y_8	Maximum live load shear including impact in interval 1	4.45 kN (1 kip)
Y_9	Maximum live load shear including impact in interval 2	4.45 kN (1 kip)
Y_{10}	Maximum live load shear including impact in interval 3	4.45 kN (1 kip)
Y_{11}	Unit weight of concrete	156.84 kN/cu m (1 kip/cu ft)
Y_{12}	Ratio of depth of equivalent rectangular compression stress block to distance from fiber of max. compressive strain to the neutral axis, a_1	—

Note: Intervals 1, 2, and 3 are defined in Fig. 3(b).

Table 3: Design variable for X and Y (Frangopol et al. 1997)

The conclusions of this study are the deterioration of the reliability of reinforced concrete structures over time due to corrosion is larger for moment than for shear strength. The authors say that the proposed design can help maintain the reliability of RC girders and note that when taking into account the total material and expected lifetime cost it is required to design for longer expected lifetime reliability. The study also emphasizes the need for further research in order to achieve optimization of the design model.

The same fact holds true for the research done in this paper since the production of the model can be considered as quite complicated. For the purpose of creating an example of the methodology required to achieve the goal of identifying corrosion risk over a general area, this paper takes into account a variety of researches from different people with at times

different opinions, therefore in order for the model to achieve the goal of being usable later on further research, optimization, testing and authentication is needed.

3.1.7 Deterioration of reinforced concrete structures

The deterioration of reinforced concrete structures is a matter addressed in a research by P. Thoft-Christensen (Thoft-Christensen 2000). The study performs a stochastic modeling of the deterioration of reinforced concrete structures proposing that for the correct representation the physical and chemical properties of the concrete must be adequately comprehended. Inside the study the crack width is investigated in relation to the corrosion of steel and a new service life definition is proposed based on the width of said crack width. Thoft-Chrestensen considers the service life of a building to be the result of the equation:

$$T_{service} = T_{crack} + \Delta T_{cr} = T_{corr} + \Delta t_{crack} + \Delta T_{cr} \quad (22)$$

where: $T_{service}$ = Service life

T_{corr} = Initiation time for corrosion

Δt_{crack} = Time from corrosion initiation to corrosion crack initiation

ΔT_{cr} = Time from initial cracking until a critical crack appears

by implementing other known equations into the service life equation the equation becomes:

$$T_{service} = \frac{w_{service} - w_0}{\gamma c_{corr} i_{corr}} + T_{crack} \quad (23)$$

where: $w_{service}$ = Critical serviceability corrosion crack width

w_0 = Initial crack width

γ = factor from Andrate et al., 1993 experiments ranging from 1.5 to 5

c_{corr} = Corrosion coefficient

i_{corr} = Rate of corrosion

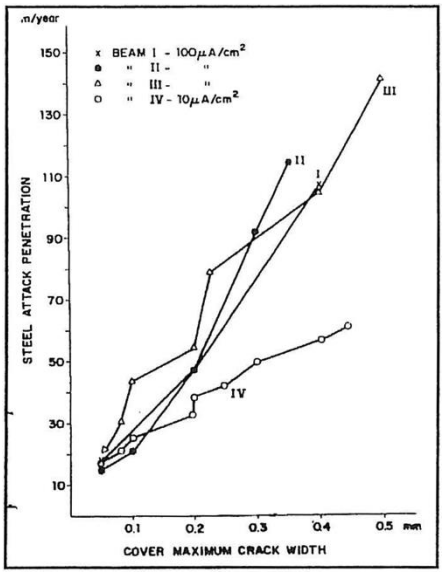

Figure 18 :Loss in rebar diameter in relation to crack width (Thoft-Christensen 2000)

The conclusions of this study are that the modeling of corrosion can be divided into the penetration of the corrosion inhibitors within the concrete, and then the evolution of corrosion products with the effects these products have on the concrete.

The same as the other researches, this research can give greater insight of how to model the corrosion risk in a general area, and what factors affect this corrosion.

3.1.8 Initiation of steel corrosion at critical carbonation depth

The effect of carbonation on steel corrosion rate is a matter that has seen a lot of varying opinions as indicated in a study by Hussain and Ishida (Hussain and Ishida 2009). In order to research this matter further Hussain and Ishida conducted experiments for the process of carbonation in concrete and the initiation of steel corrosion, while measuring the carbonation depth, the corrosion potential and the corrosion mass loss. The study also developed an electrochemical corrosion model for carbonation which is compared to results from experiments in order to validate its authenticity. Also the relation between the depth of carbonation and the corrosion potential is examined by using the results from the experiments in conjunction with the carbonation depth and half-cell potential. The real reason for these experiments in this particular study is to identify the critical carbonation depth by observing the behavior of the carbonation depth to corrosion potential profile. In the study some observations are noted beginning with the observation that the corrosion due to carbonation won't initiate unless the carbonation in the concrete reaches a certain critical distance from the rebar. Also it is observed that the half-cell potential values rise again after the carbonation

reaches the rebar. The rate of corrosion in carbonation induced corrosion is relatively slow when compared to chloride induced corrosion, however it is greatly influenced by the relative humidity. The study claims to validate these facts through the experiments and the carbonation induced electrochemical corrosion model. The equation used for the enhanced electro-chemical model to predict the carbonation induced corrosion rate in this study is:

$$D_{dCO_2} = \frac{\emptyset D_o^g}{\Omega} \frac{(1-S)}{1+\frac{l_m}{2(r_m - r_t)}} \quad (24)$$

where: D_{dCO_2} = Diffusion coefficient of dissolved CO_2 in a porous medium (m^2/s)

Ø = Porosity of the porous media

Do^g = Diffusivity of CO_2 in a free atmosphere ($=1.34x10^{-5}$)

Ω = Average tortuosity of a single pore as a fictitious pipe $(=\pi/2)^2$

S = Degree of saturation of the porous media

l_m = Mean free path length of a molecule of gas (≈352pm)

r_m = Average radius of unsaturated pores

r_t = Thickness of the absorbed water layer in the pore with radius r_m

The study concludes saying that the values of the half-cell potential fluctuate according to time and carbonation depth for corroding rebars. These values for the half-cell potential range between -180mV CSE to -475mV CSE. The critical carbonation depth that is required for the initiation of corrosion on the construction steel was evaluated to be at 80% of the total depth of the cover that the reinforced concrete has. For a relative humidity of 55% to 60% it was calculated that the corrosion rate is 0.325μA/cm^2, which validates the opinion of corrosion rate due to carbonation is much lower when compared to corrosion rate due to chloride ions. The model suggested is considered to reasonably predict corrosion behavior for relative humidity of 55% to 60% at a carbonation level of pH 8.0.

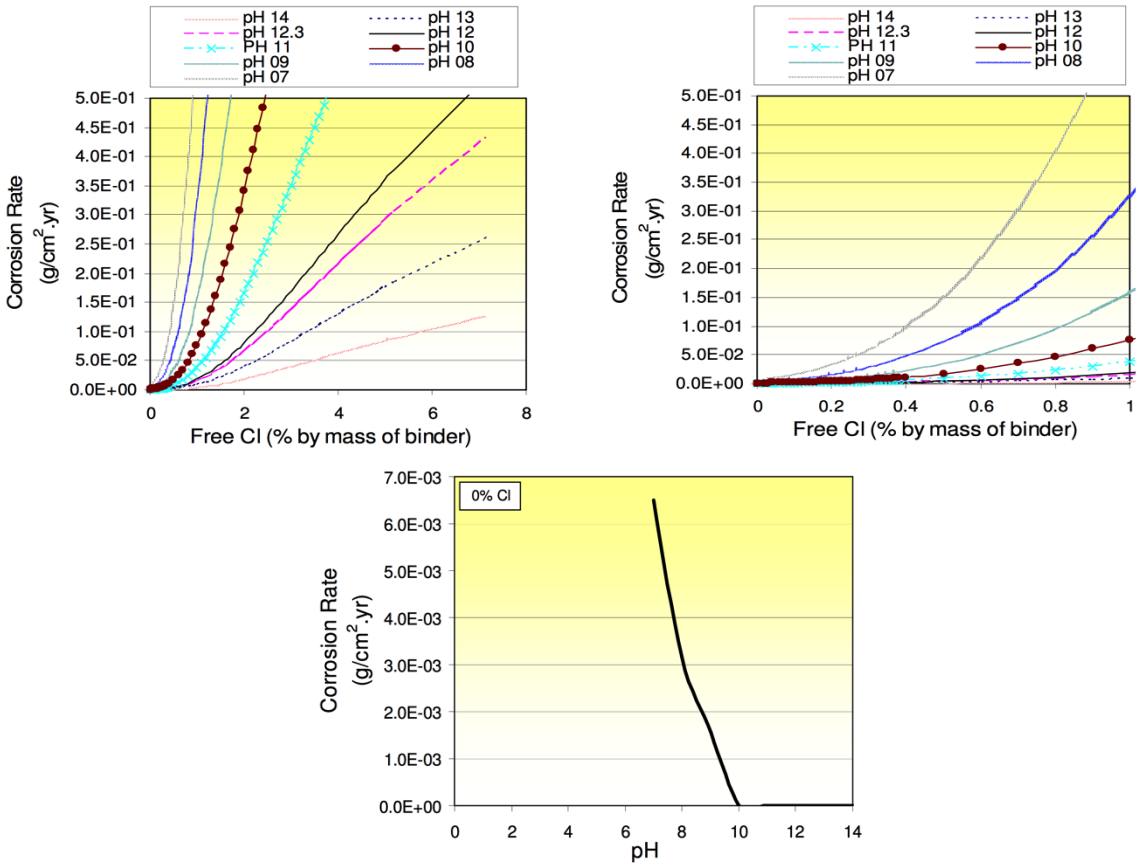

Figure 19: Corrosion rate (Hussain and Ishida 2009)

The model used in the study for the prediction of corrosion rate due to carbonation is one of the important modules of the equation needed to attribute corrosion rate over a large area by the use of GIS tools.

3.2 The mathematical model

The studies mentioned and analyzed before can give as a better understanding of the mechanism of corrosion. The main aim of this paper is to determine how the probability of corrosion interacts with the various obtainable data from a general area, and how by inputting that data in programs like GIS tools can help as have a better image of what areas can be considered as high corrosion risk areas. For that to be achievable a mathematical model that combines accurately all of the data that is obtained is necessary. The mathematical model that this paper will use is by no means something that should be used or considered as accurate or a real representation of the probability of corrosion. The model is used simply as to allow for the creation of a starting methodology that will potentially, after a lot of testing, comparison, experimentation and refinement lead to the realization of a model able to give to engineers

accurate feedback of what is going on with the area they are working on when corrosion is considered.

3.2.1 The base for the model

The general idea for the model is to create a mathematical equation that by taking into account all the data that affects corrosion will give as the end result the risk of corrosion at a certain point on a map. The best way to approach this problem would be to identify every parameter that influences corrosion in any way and then isolate each individual aspect of these parameters in different equations, which have as a result their influence on corrosion as a probability of the risk of corrosion. Then to identify the relative influence that each of these equations have on corrosion when compared to each other in order to create coefficients in a way that give the equations with more influence greater weight than that of the other equations. Each equation then must be normalized so as to achieve the same range of results for all of these equations and in order to be able to somewhat relate the result of each equation to the other results. When trying to create the model we can write the equation in a general and simplified form like:

$$R = a\left(\sum_{j=1}^{n} b_j \frac{c_j N_j}{\sum_{k=1}^{n} c_k N_k}\right) \tag{25}$$

where: R = The risk of corrosion

a = Multiplication factor in order to create a range of desirable values

b = Coefficient for the weight of each factor

c = Coefficient for each individual equation

N = Equation of each factor concerning corrosion

The equation suggested above is not proven or validated in any way. However for achieving the purpose of this paper which is to suggest a new methodology for acquiring data concerning corrosion, it will be used in conjunction with other equations from the above mentioned studies in a way so as to make a point of the possibilities of expanding and furthering this methodology. The data that will result from this paper will most likely be inaccurate and should not be used as facts. Also due to not phasing through the steps that are mentioned above of isolating and testing each and every parameter of the factors affecting corrosion, with the reason being that much time and research is needed in order to achieve that, the results may not be satisfactory.

3.2.2 The creation of the model

In this stage a rough equation will be created depicting the corrosion risk in a specific point. For this equation data from two different studies mentioned above will be used so as to create a sample of what the equation will likely look like. The studies used are for the effect of carbonation on steel corrosion rate (Hussain and Ishida 2009) where in general the higher the value gained from the equation the greater the risk of corrosion. The study used for the prediction of time from corrosion initiation to cracking (El Maaddawy and Soudki 2007) where the lower the value given by the equation, the greater the risk of corrosion.

$$D_{dCO_2} = \frac{\emptyset D_o^g}{\Omega} \frac{(1-S)}{1+\frac{l_m}{2(r_m-r_t)}} \tag{24}$$

$$T_{cr} = \left[\frac{7117.5(D+2\delta_0)(1+v+\psi)}{iE_{ef}}\right]\left[\frac{2Cf_{ct}}{D}+\frac{2\delta_0 E_{ef}}{(1+v+\psi)(D+2\delta_0)}\right] \tag{6}$$

The combination of all these equations with the model suggested as the base for this model is result in:

$$R = 255\left(0.6\frac{\left[\frac{PD_o^g}{\Omega}\frac{(1-S)}{1+\frac{l_m}{2(r_m-r_t)}}\right]}{Q}\right) + \left(0.4\frac{\left[\frac{1}{\left[\frac{7117.5(D+2r_m)(1+v+\psi)}{iE_{ef}}\right]\left[\frac{2Cf_{ct}}{D}+\frac{2r_m E_{ef}}{(1+v+\psi)(D+2r_m)}\right]}\right]}{Q}\right) \tag{26}$$

$$\psi = \frac{D'^2}{2C(C+D')} \tag{27}$$

$$Q = \left[\frac{PD_o^g}{\Omega}\frac{(1-S)}{1+\frac{l_m}{2(r_m-r_t)}}\right] + \left[\frac{7117.5(D+2r_m)(1+v+\psi)}{iE_{ef}}\right]\left[\frac{2Cf_{ct}}{D}+\frac{2r_mE_{ef}}{(1+v+\psi)(D+2r_m)}\right] \quad (28)$$

where: R = Risk of corrosion

P = Porosity of the porous media (3% - 22%)

Do^g = Diffusivity of CO_2 in a free atmosphere ($1.34x10^{-5}$)

Ω = Average tortuosity of a single pore as a fictitious pipe $(\pi/2)^2$

S = Degree of saturation of the porous media (0% - 100%)

l_m = Mean free path length of a molecule of gas (352pm)

r_m = Average radius of unsaturated pores (1nm - 1cm)

r_t = Thickness of the absorbed water layer in the pore with radius r_m ($<r_m$)

D = Diameter of the steel reinforcing bar (6mm - 30mm)

v = Poisson's ratio (0.18)

i = Current density ($10\mu A/cm^2$ - $1000\mu A/cm^2$)

E_{ef} = Effective elastic modulus of concrete (22 - 33 MPa)

f_{ct} = Tensile strength of concrete (3 - 7 MPa)

C = Concrete cover (20mm - 70mm)

The resulting equation will now be used in programs such as GIS tools in order to find the corrosion risk for specific points on a map. Then with the tools provided the corrosion risk map will be created that will show for the general area of the map containing the points in which areas corrosion in structures is more likely to occur.

4 GIS Methodology

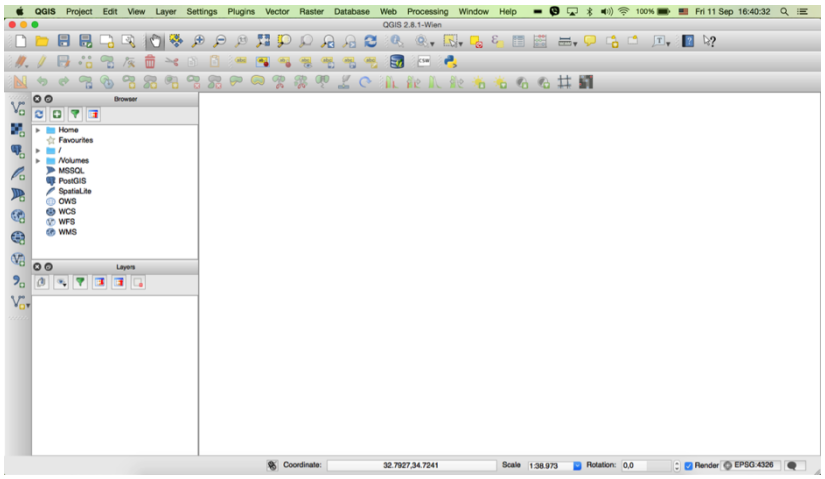

Figure 22: QGIS software interface

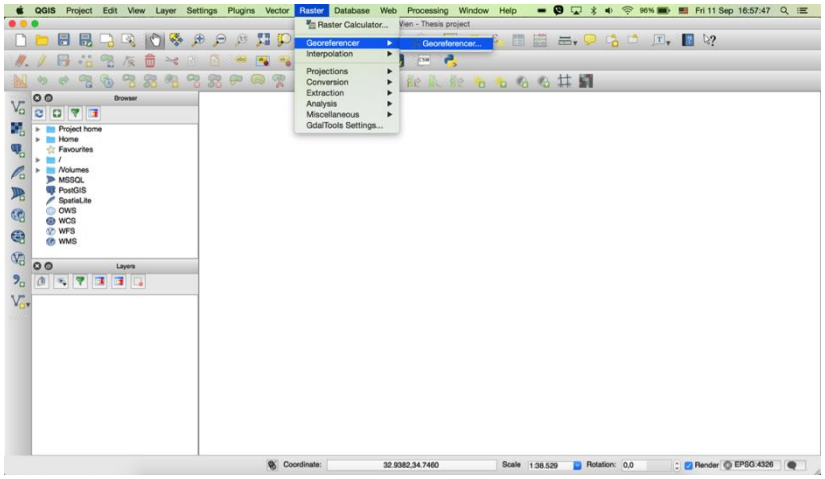

Figure 21: Georeference of the map

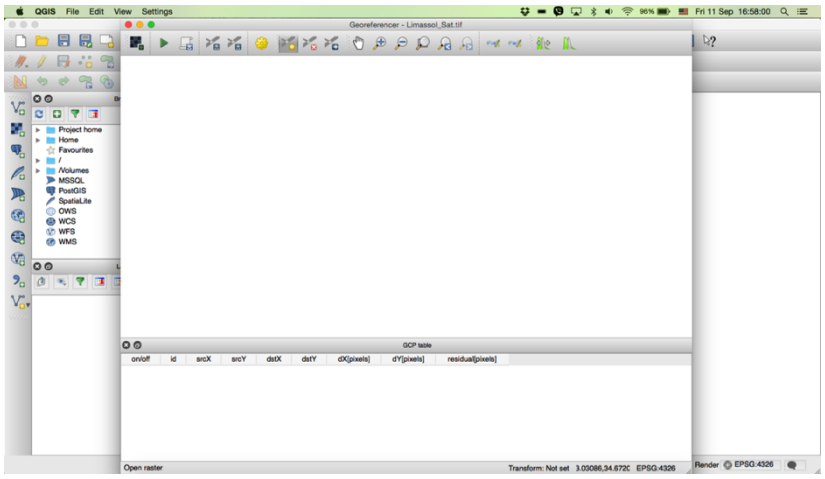

Figure 20: Georeference interface

For the purpose of using the equation to create a risk of corrosion map, the use of GIS software is needed. The specific software used in this specific paper is QGIS since it is an open software and accessible to everyone. The purpose of using GIS tools is to be able to concentrate all of your data in single software so as to be easier to organize and analyze it to receive the results you need. The first thing you will need when trying to create the risk map is the map of the area of interest. That map then has to be modified through the georeferencer in order for the places depicted in the map to have the correct coordinates. That is vital since in the case that you are using a variety of different maps or you wish to publish or keep the data it will allow you to relate the data you have geodetically to other data.

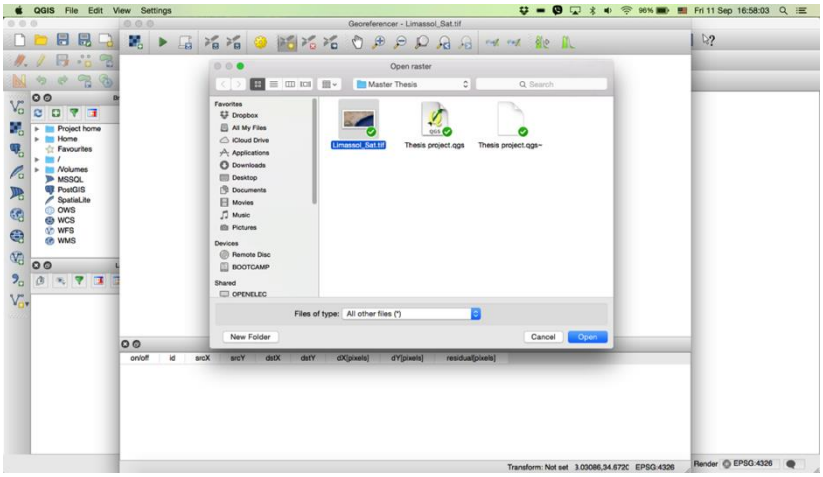

Figure 23: Opening the map you need

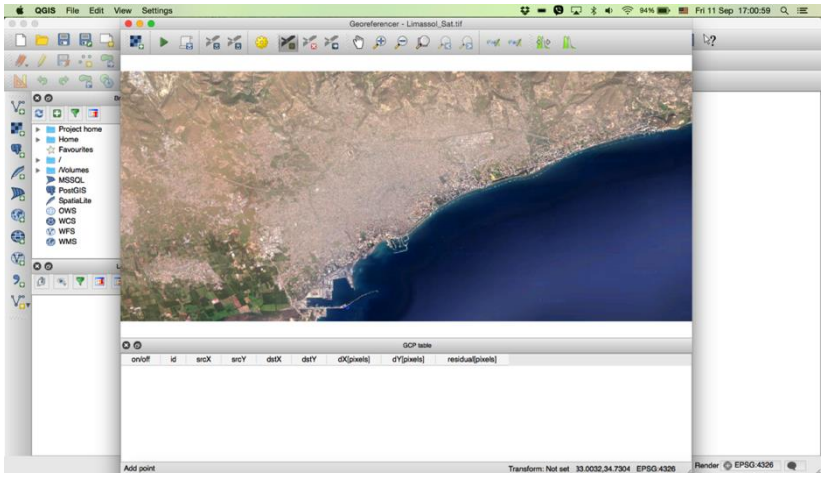

Figure 25: Open the add points tool

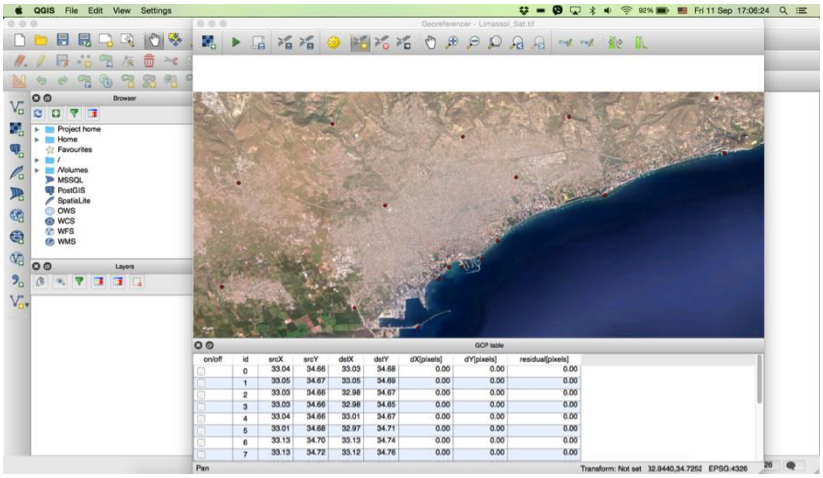

Figure 24: Add known points to the map and their coordinates

The way to georeference a map is by adding it to the georeference tool, and then by using the point tool to add points on the map. It is best to have the points spread over the entire map of concern instead of being added in only one area of the map. It is also required that the coordinates of these points are known since you must manually input them for each point. By starting the process of georeference the software will stretch the map in a way that will put the points you noted graphically on the map above the points you noted by writing the coordinates.

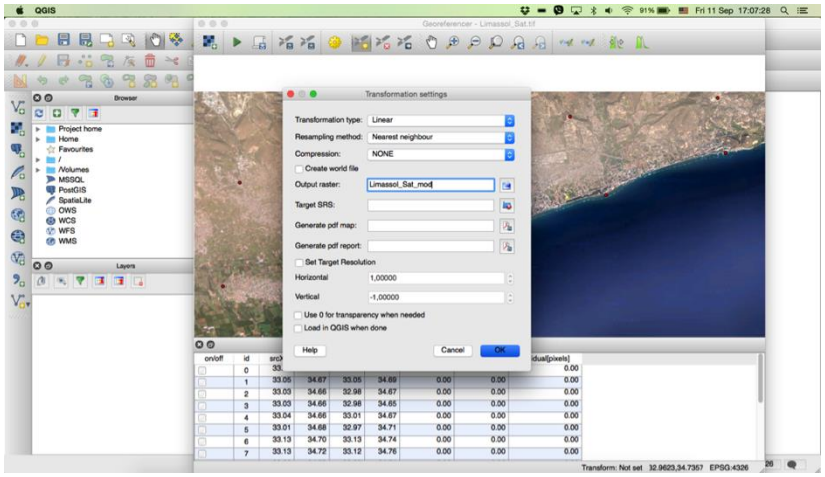

Figure 28: Save the georefernced now map and choose the transformation settings you need

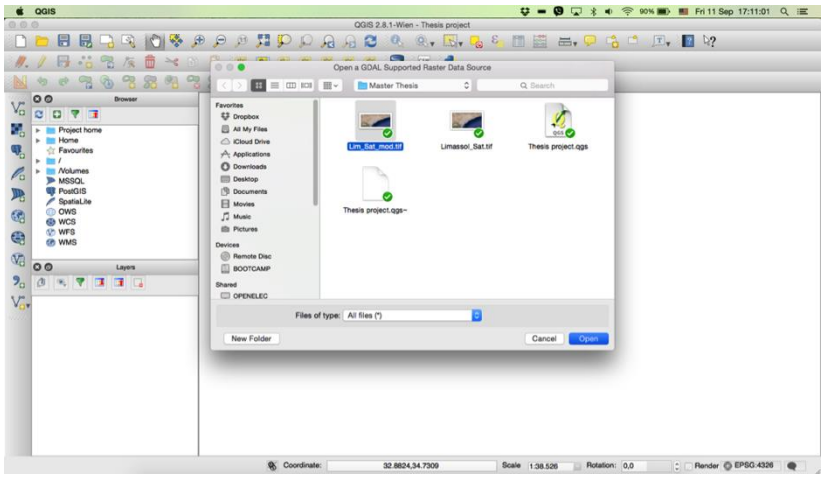

Figure 27: In the QGIS interface add the georeferenced map

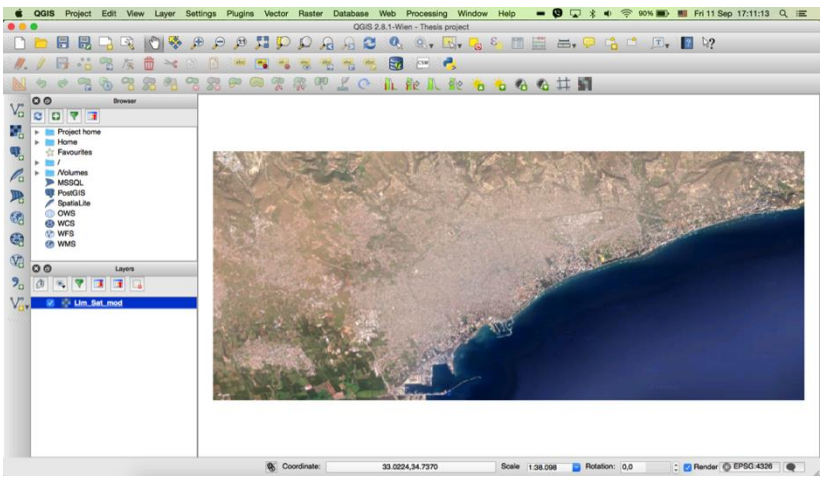

Figure 26: Zoom to the map

The georeferenced map in reality is transformed by using an equation of your choice for cases where the simple linear type of transformation is not considered as representative of the area of concern. For the paper we will use the linear type of transformation since it cannot be ascertained where another type of transformation is more appropriate for this case. The resulting map from the georeference has to be saved as a new map and it is that map that will be used in the main interface of the program in order to make the risk map that is the purpose of this paper.

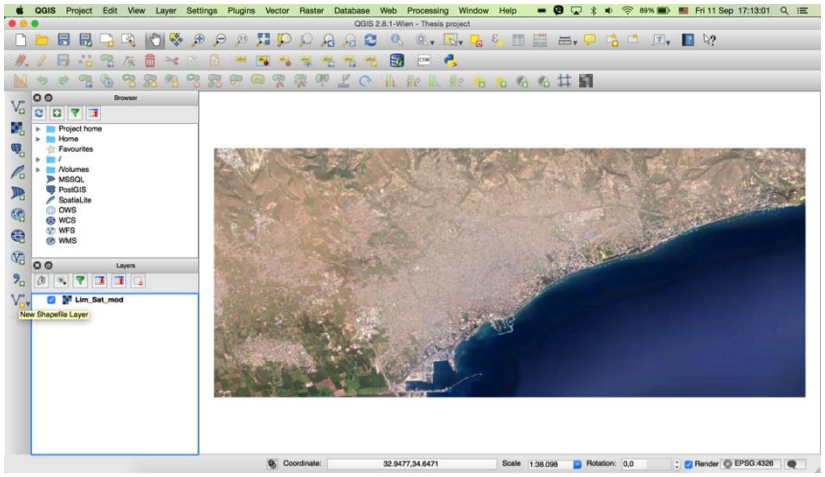

Figure 31: From the toolbar select the new vector layer

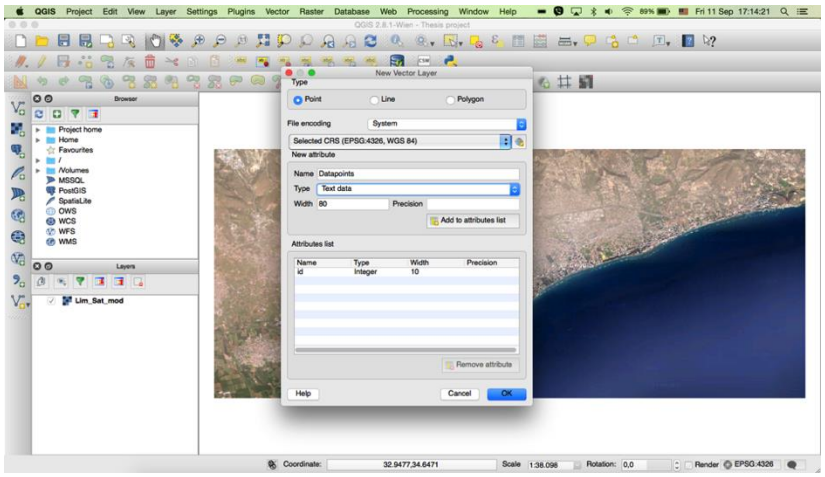

Figure 30: Set The type of the layer as point

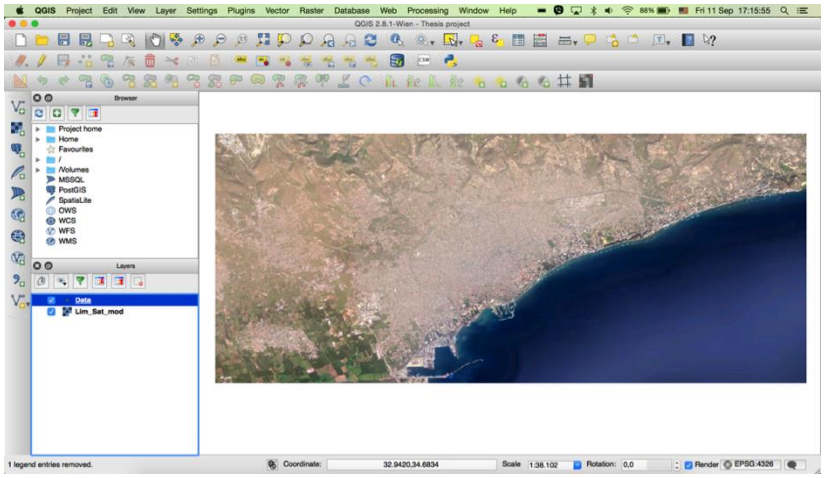

Figure 29: From the sidebar select the new layer

After georeferencing the map you will use, you have to add it to the main interface of the program in order to be able to relate your other data to it. For the goal of this paper there are a lot of different ways to achieve the desirable result but since the amount of data and time available is limited the decision was to create a point layer, or in other words a database that relates only one specific point on the map to other data. The layer has to be saved as a different set of files from the main file that the project is saved. The layer will be used to represent data that is fabricated in order to satisfy the needs of this study. The data will represent factors that influence the corrosion of steel reinforcement in concrete and how the risk of corrosion increases due to these factors.

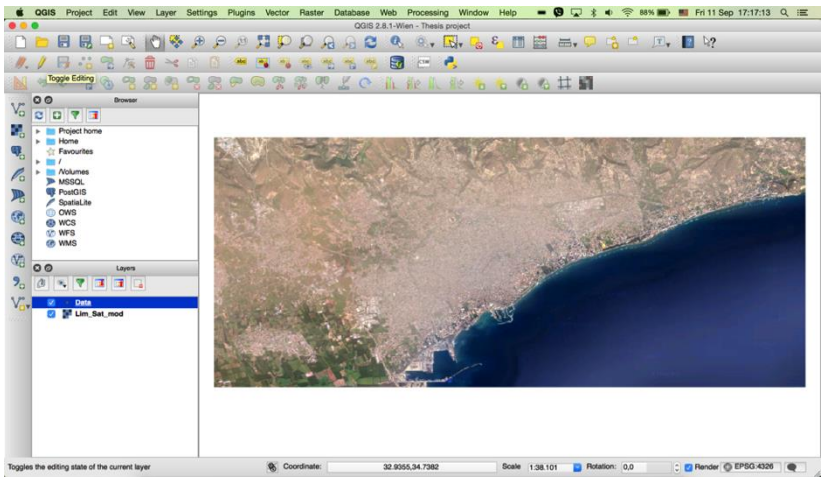

Figure 34: Toggle the editing button

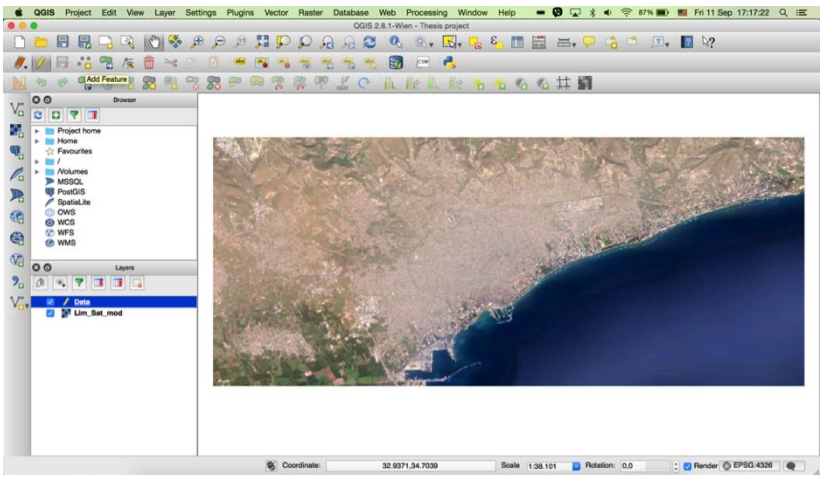

Figure 32: Select the add feature button

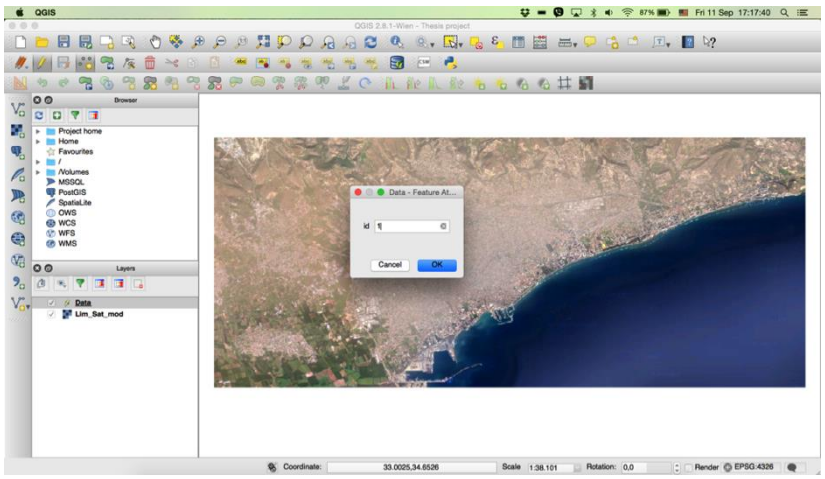

Figure 33: Id each point that you will add to the map

Normally the data should be real and acquired through trustworthy sources or measured by the same person that will use that data in the program. However in order to cover such a large area as the one mentioned would require a substantial amount of human power or of equipment or even both. Since the data is spread over an area as big as the area we would like to study, it is usually at the level of a whole city, therefore making it impossible to gather the data without help from sensors and satellites. The data usually needed for depicting corrosion concern distances, temperatures, wind flow, humidity and others.

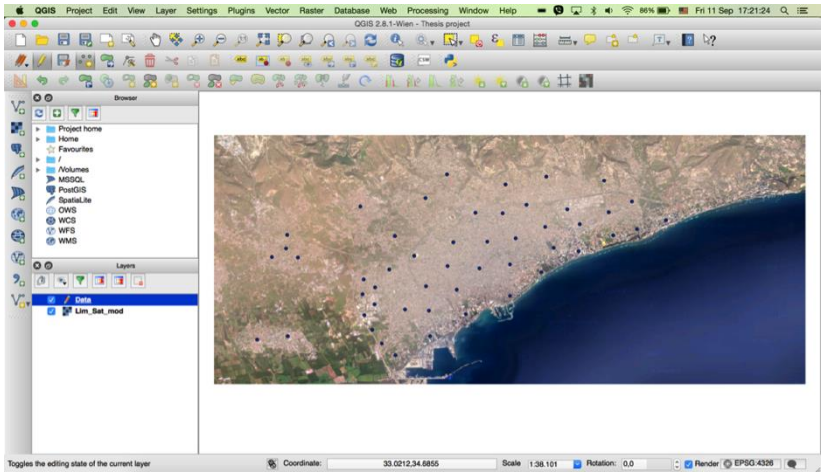

Figure 37: Spread the points on the area of interest

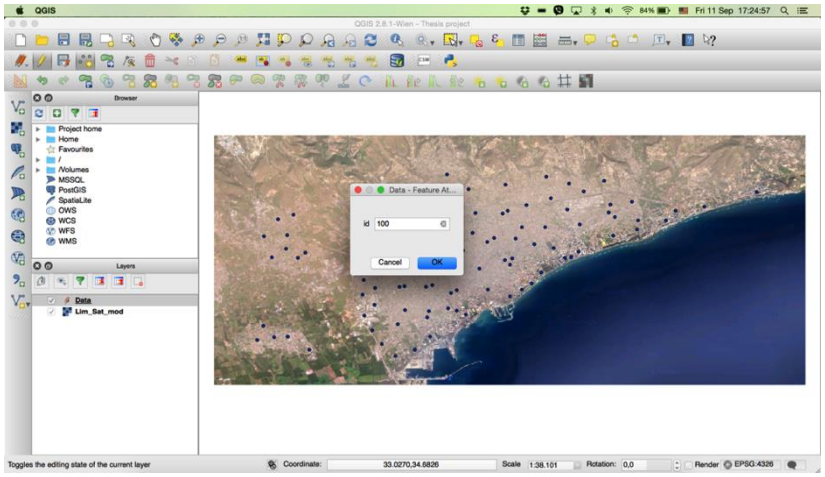

Figure 36: The points added were 100

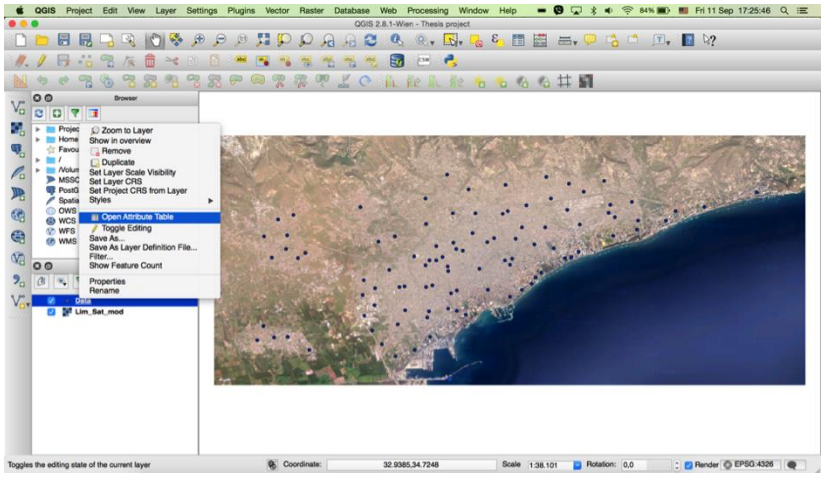

Figure 35: Open the attribute table of the Points layer

By spreading the points that will carry the fictional data over the whole area we can get a better image of the real situation when the corrosion risk map is generated. If the data come from sampling then the people doing the sampling should follow the same line of thought and get samples from a wide range of area rather than from only a limited number of places. In this paper the number of fictional points created is 100. It was decided that 100 points of data would be sufficient to create the risk corrosion map, however the number is subject to change and the number of points needed varies greatly with the are of interest.

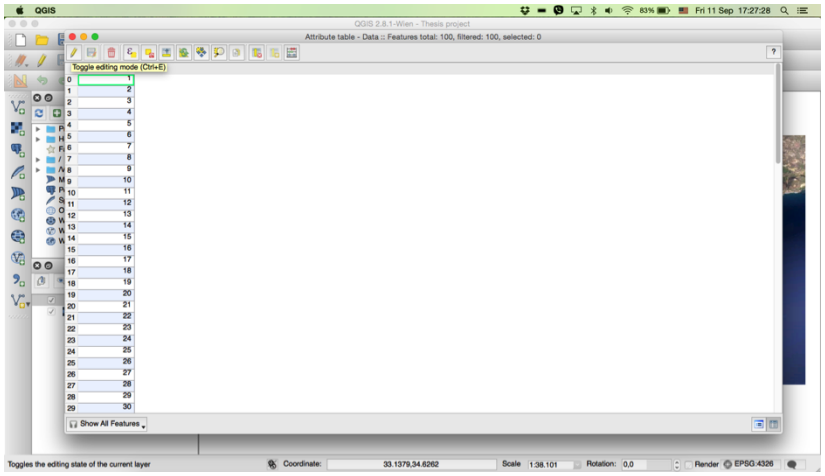

Figure 40: Toggle the attribute table editing button

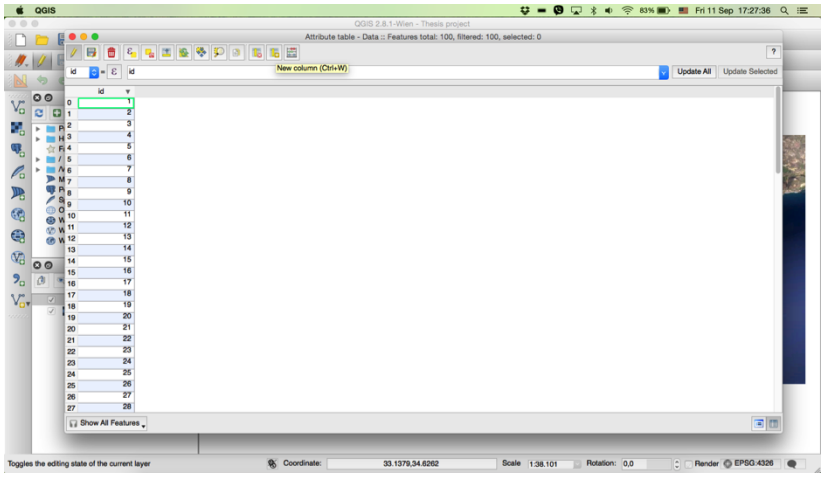

Figure 39: Press the add column button

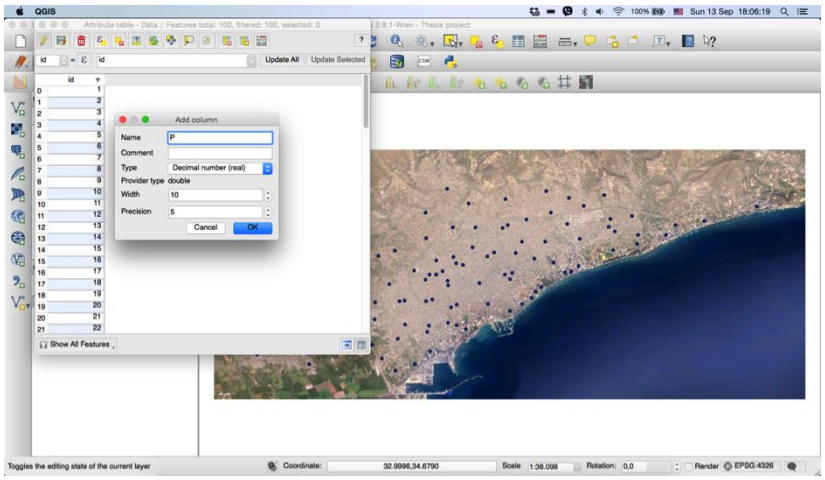

Figure 38: Name and choose the correct settings for each required field

The next step in the program is to open the attribute table of the point layer. The attribute table contains a column filled with the id that we gave to each point of the layer when we were placing them. This is where we can fill the layer with all the data we wish to place on the points. For that we need to enable the editing of the attribute table by toggling the editing button. Then we can create as many columns as we need to get the corrosion risk for each one of these points. For each column we must specify the name and the type of fields that specific column has. For the case of this methodology almost all data are proclaimed as decimal numbers.

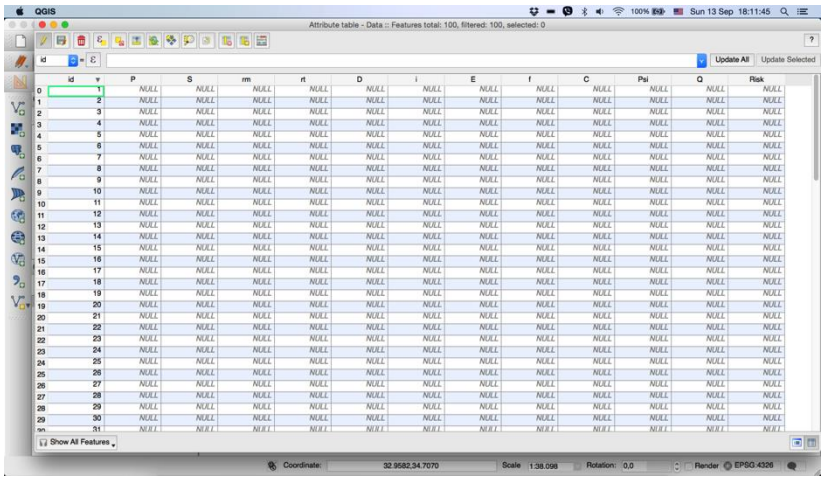

Figure 43: Add all the columns you need

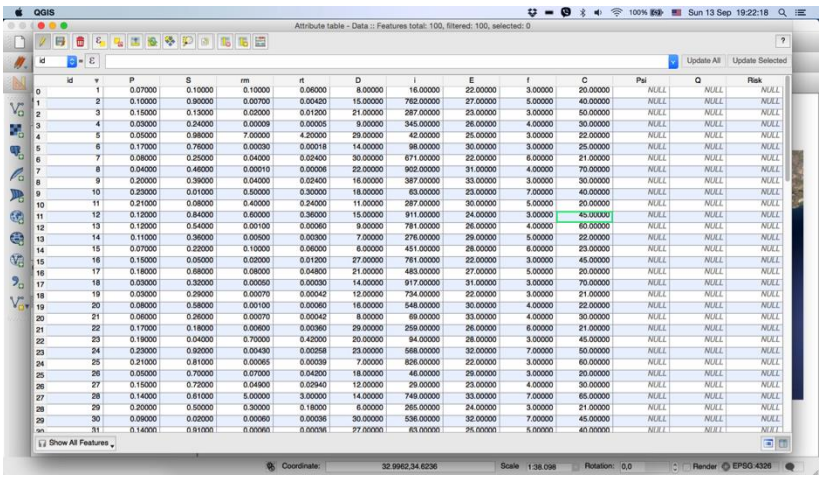

Figure 41: Fill the columns with your data

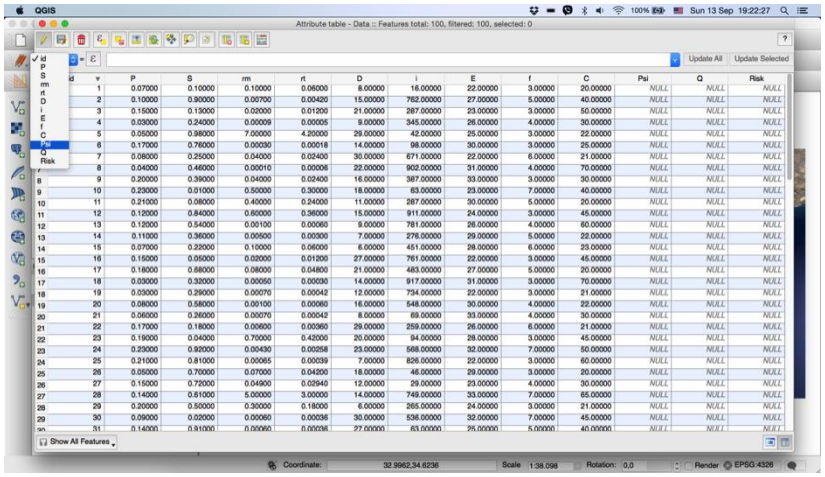

Figure 42: For filling fields with equations, choose the field from the dropdown menu

The columns added are one for each one of the factors that we consider as important enough to affect corrosion and one more for each one of the equations that will be calculated. In the methodology 13 columns are created of which 4 are equations and the other 9 factors of these equations. Each cell is filled with the fictional data that is mentioned above. All fictional data must of course obey to the rules and constraints that the authors of these equations have noted.

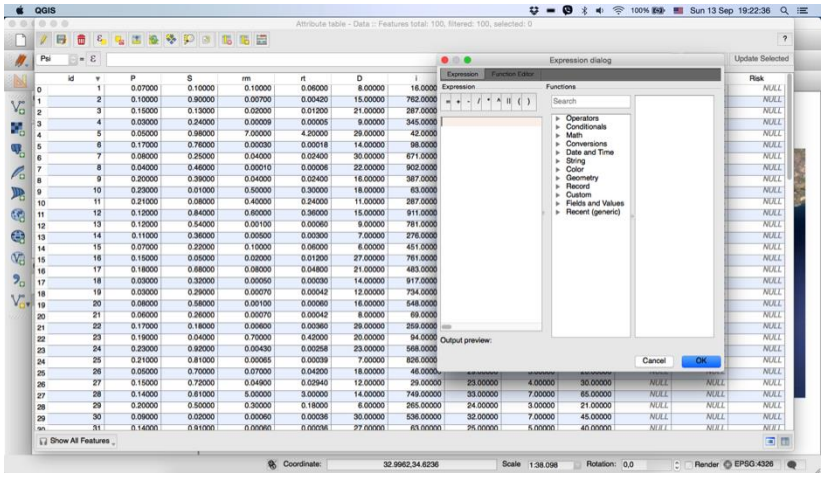

Figure 46: Open the equation tool

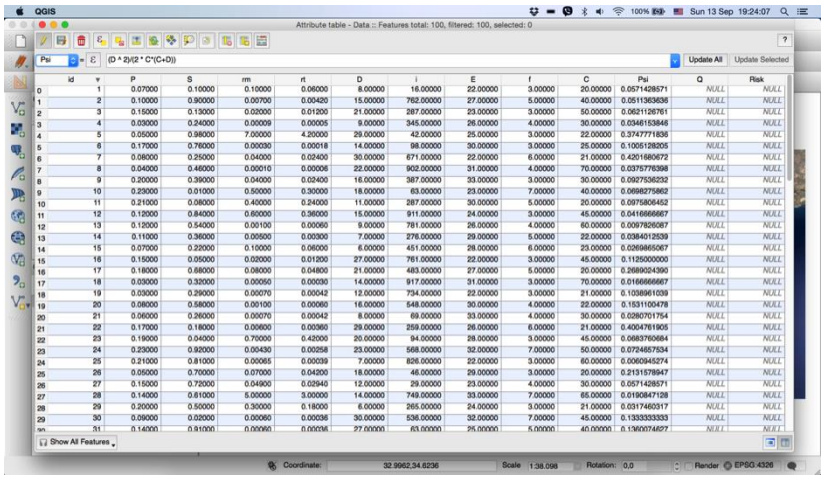

Figure 44: Write the equation

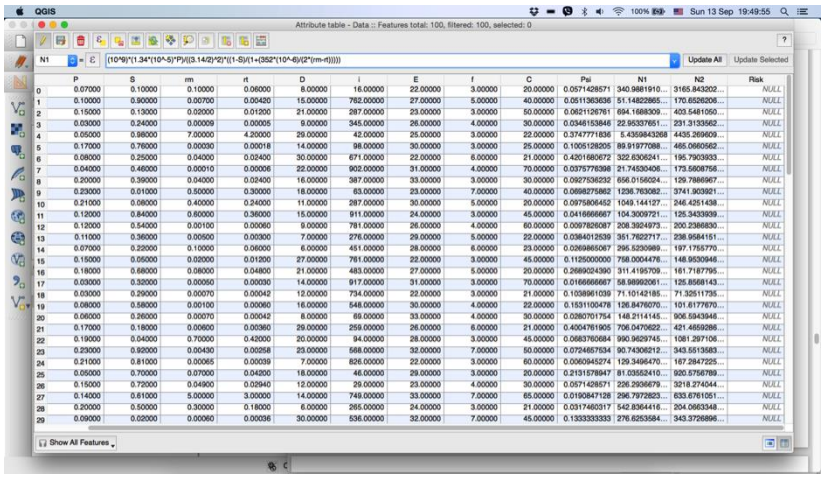

Figure 45: After writing the equation update all fields of the column to get the results

For the columns created for the use of equations you must first choose which exact column you want the result of the equation to appear to. Then you can open the equation tool and use the symbols to create the equation you need. For the case of this methodology two different equations were used as mentioned also in the previous chapter. After writing the equation you can use the update button in the attribute table to update all the cells of the column with the equation you wrote and show the results. This procedure is used for all of the equations in the methodology.

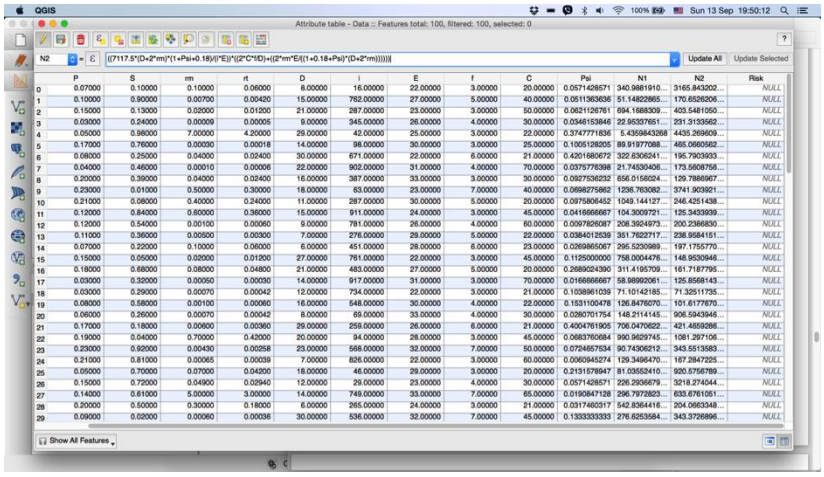

Figure 49: The individual equations are filled

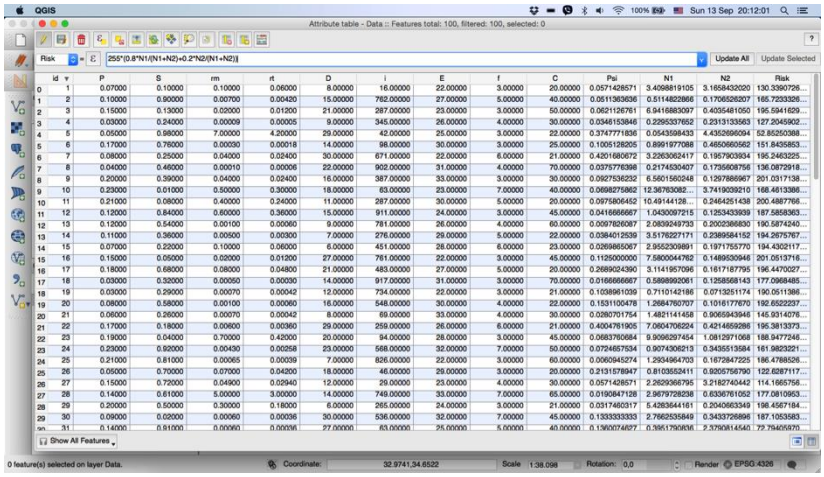

Figure 47: Finally the risk equation is written to get the risk values we need

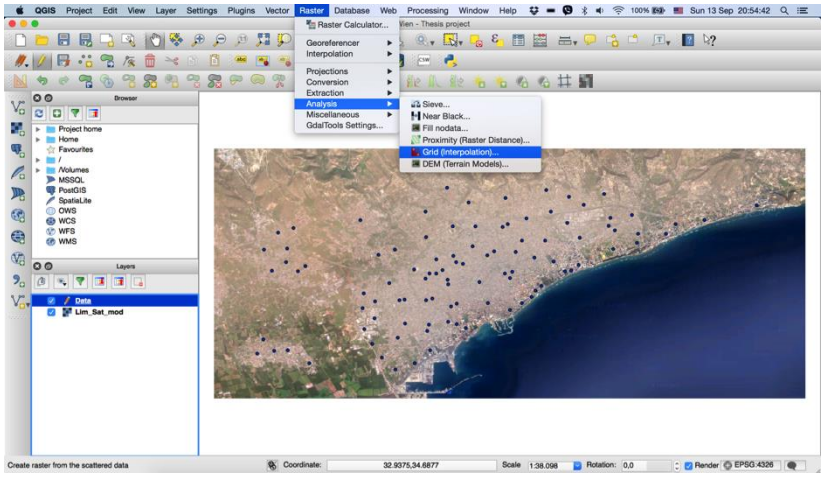

Figure 48: Open the tool for grid analysis

The last equation and the main reason for creating the point layer is the risk of corrosion, or the probability of risk occurring in structures. After getting the values for the probability of corrosion in structures we can actually ignore all other data since the only reason for creating the layer was to correlate the map of the area and the coordinates to these values of corrosion risk. When we have this correlation of topography and values we can create a raster file that will show a different tone of color for every value of corrosion risk in the attribute table and then through interpolation will fill in the empty spaces so as to create a grid.

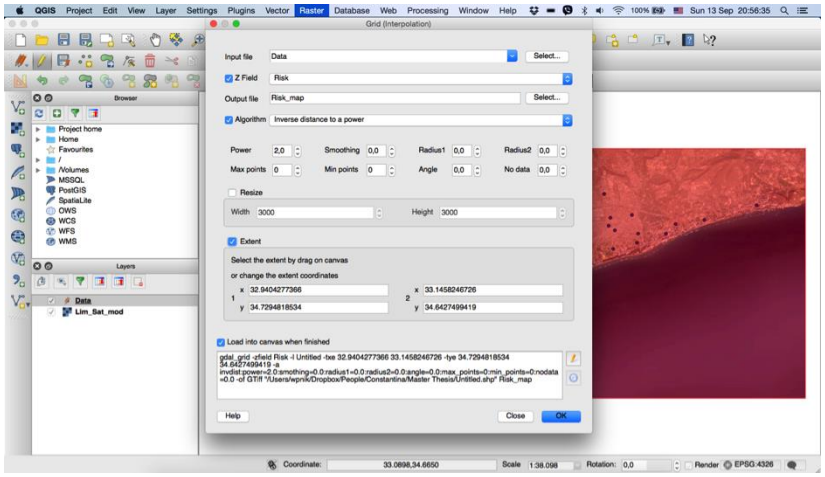

Figure 52: Fill the fields and set the coordinates for the resulting raster file

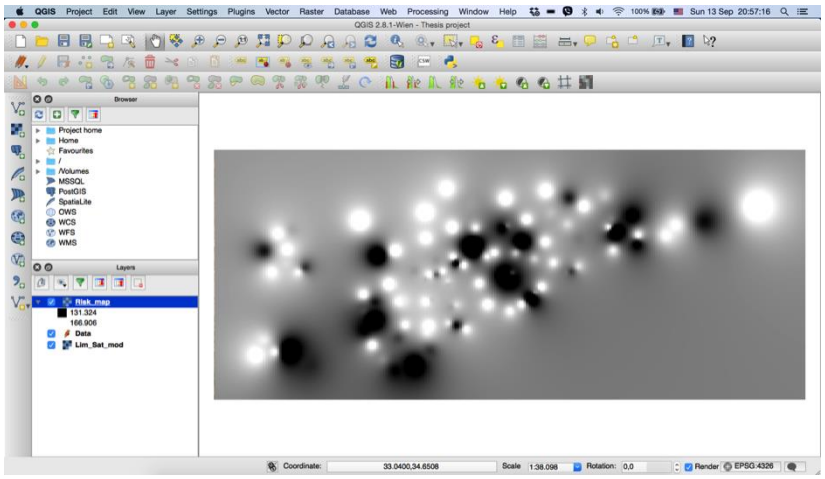

Figure 51: The result from the analysis

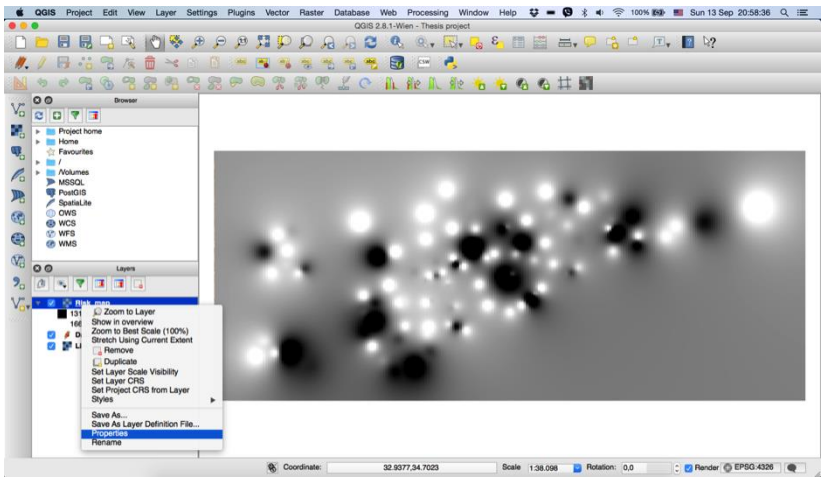

Figure 50: Go to the properties of the resulting image

By choosing the analysis as a grid from the program we must then make a few other choices. First we enable the custom values for the z field and set corrosion risk as the value. Next we choose the algorithm we wish to create the grid with and the range of coordinates we want the newly created map to expand to. The result of the analysis can be seen as a black and white image with a variety of grey tones. This image though does not give us the information we need about the risk of corrosion in the area since we do not know what each tone of grey is meant to represent.

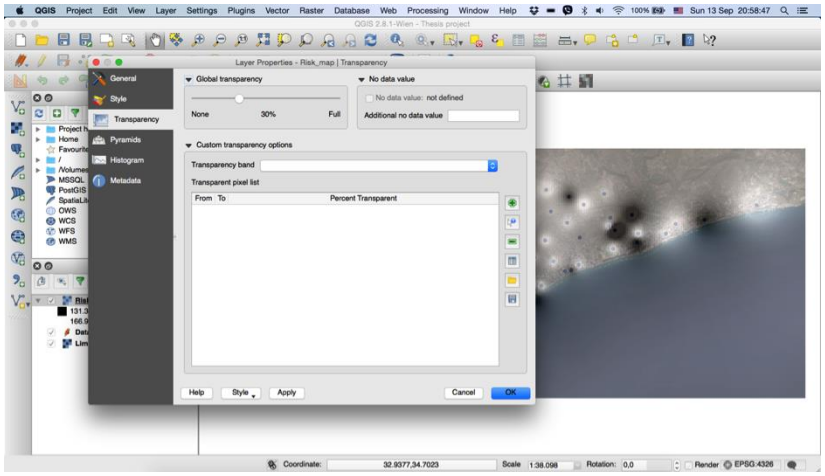

Figure 55: Set the transparency to a higher level to be able to see the image in relation to the map

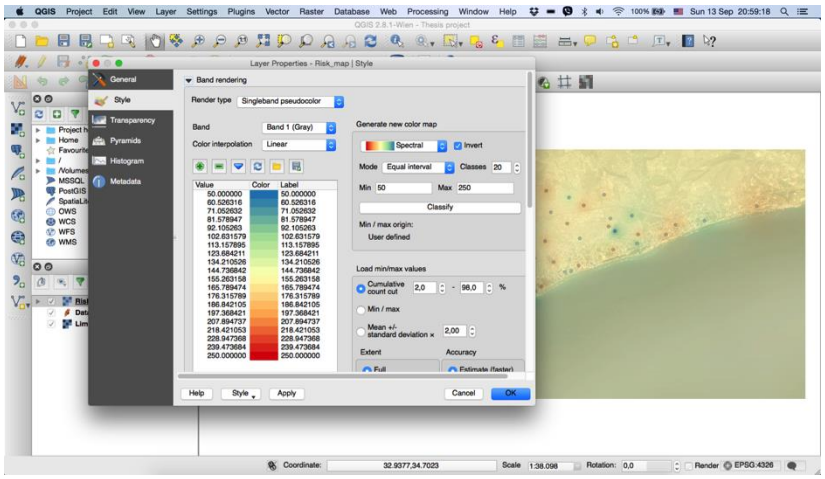

Figure 54: Change the style of the image

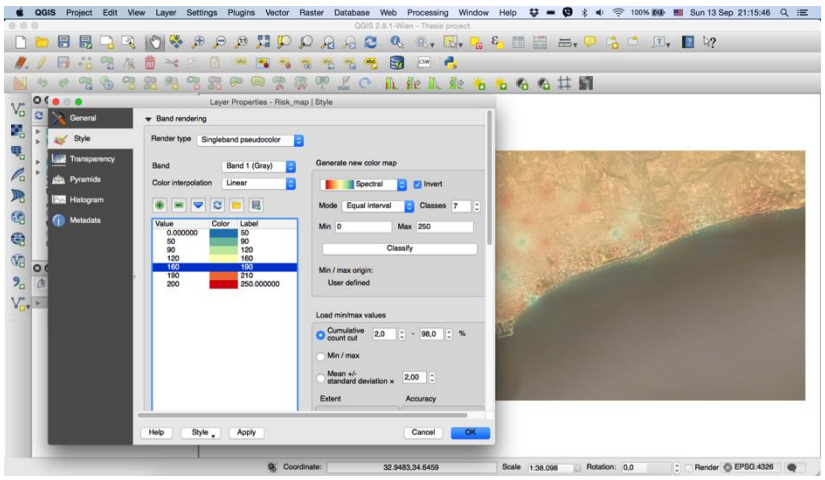

Figure 53: Reclassify the image in a way to make the risk map more distinguishable

In order to be able to read the map that was created and understand what it really represents we need make some adjustments to the image so that the map becomes clearer. The first thing to do is access the properties of the new layer that we created. Then by going to the transparency tab we can me the black and white image transparent so that we can see the map of the area below and be able to relate each tone to the areas on the map. Now each tone of grey represents what risk of corrosion value is in each cell of the grid we created through the analysis. However we can reclassify the data in a different way in order to set what we consider dangerous or safe when concerning corrosion on the map that we created. By reclassifying the data we can get a better image of what concerns us as engineers.

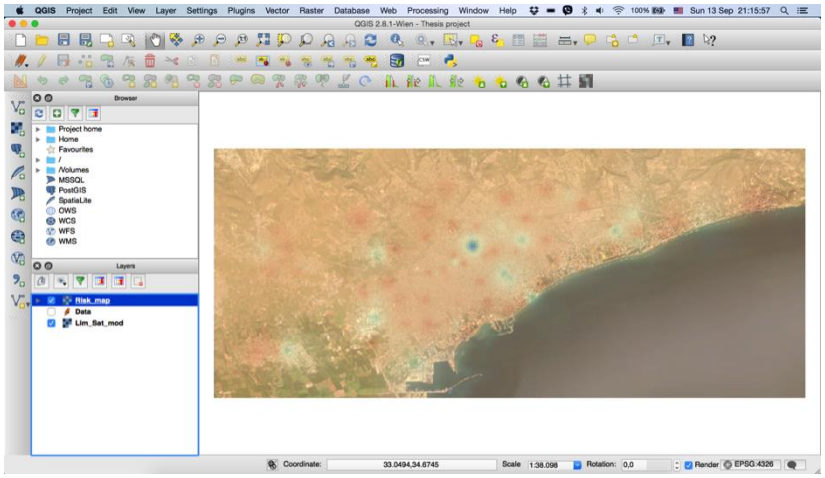

The result of this process is a map of the risk corrosion in the area with deep red being the most dangerous areas and with deep blue the most safe areas. The map that was created can be seen in the annexes of the paper.

Figure 56: The end result can be saved as a new map

The main reason this method of creating the map was chosen is due to the lack of data and time. The result of this methodology is not accurate since all data was fictional and random instead of real results from measurements. A better way of creating the map would be by isolating each parameter within the equations that will be used to depict the corrosion risk. Then by gathering the data that is needed in the form of other maps for each parameter, it is possible to extract all the information you need from each of the separate maps and then combine it to create a new map through the equations that will show the risk of corrosion in the area. This method would be much more accurate since in an image of data you can have millions of points in the area instead of just 100 points as was shown in the methodology above.

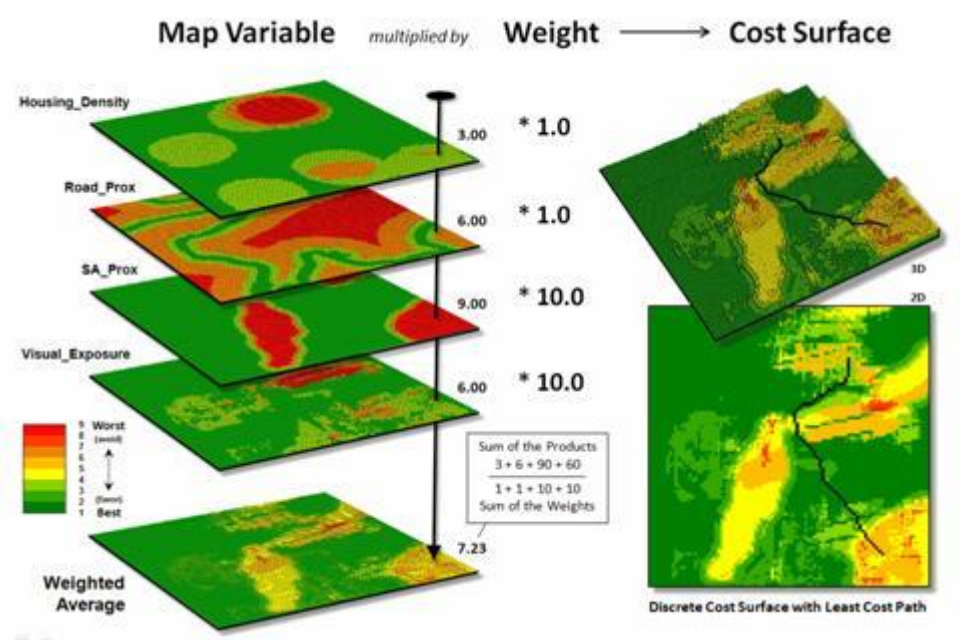

Figure 57: Combining different rasters with their specific weight to create new maps ("Map Analysis Topic 19: Routing and Optimal Paths" n.d.)

5 Results

The results of the study are shown in annexes of this paper with the attribute table and map that are exported from the GIS program. The values shown in the results hold little meaning but the purpose of this paper is not to create a map that can really represent the state of corrosion in the area, but rather to suggest a new methodology that can in the future help civil engineers. The results also are based on the assumption that the studies used were correct and also that the implementation of those studies was done correctly. Another thing that must be taken into account is the fact that the authors of these specific studies did not account for the use of GIS and therefore their equations are most probably not appropriate to be used as shown in this paper. However they can form the base for the development of the methodology and should not be discounted.

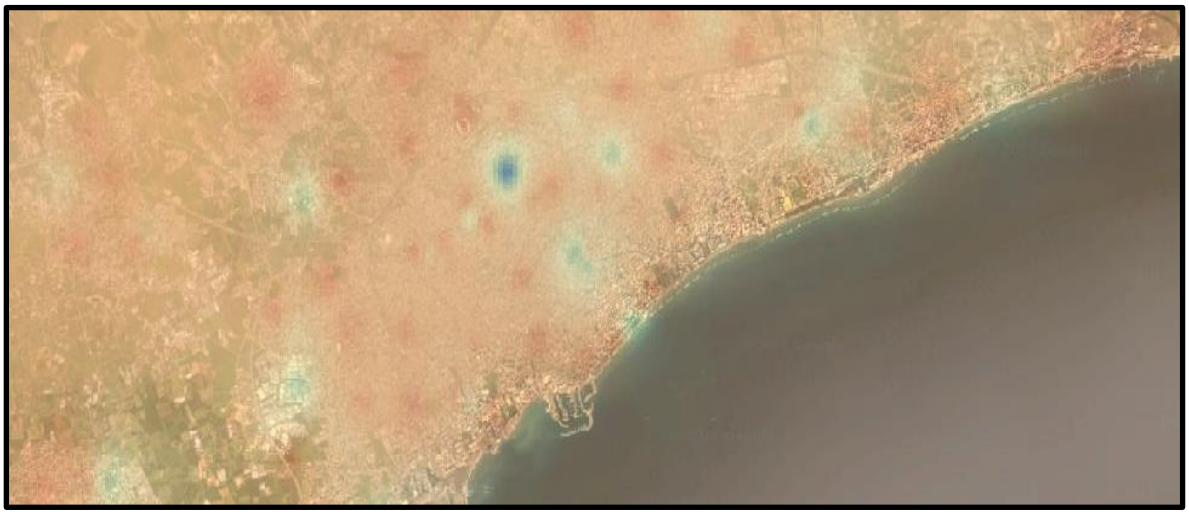

Figure 58: Resulting corrosion risk map

CONCLUSIONS

From the research done to complete this paper and the work to develop the model and methodology we reach some observations and conclusions:

1. The corrosion of steel reinforcement in RC structures is a major problem that for years researches have tried to give the optimum solution.
2. The GIS tools that exist today have advanced a great deal and can be very helpful when trying to reach the optimum solution for a variety of problems, the corrosion problem included, as long as the procedure used is correct.
3. The development of an accurate and reliable model for the prediction of steel corrosion will require a lot of time, testing and refinement and the cooperation of many different scientific fields to be completed.
4. The use of such methods as the one mentioned in the paper to create maps that showcase the probability of corrosion in a large area can help in many different ways civil engineers that work in that specific area. The design of new buildings can be influenced positively by identifying the area that they will be built as a high or low risk area for corrosion. Also by knowing the areas of high risk, preventive measure can be taken to prevent safety or economy hazards from occurring.
5. The time needed to normally take measurements on the field to ascertain whether corrosion is a problem or not usually are time consuming and expensive. This method though will be able to create results in a very small amount of time and over a much larger area without even the need of making on-site visits.
6. The large scale of the corrosion risk maps can also help the managing authorities in city planning and research about corrosion related studies.
7. The knowledge also of the corrosion risk in various areas can help engineers to more accurately provide the structures with maintenance plans in order to prevent their further deterioration.

EPILOGUE

The purpose of this paper was to investigate the risk of corrosion over a large area with the help and use of GIS tools. A methodology to achieve this purpose is suggested and an experimental situation is applied so as to create a corrosion risk map. The study aims to provide civil engineers with better and tools that can provide them with information that they are usually lacking, and are many times essential in order to correctly diagnose the situation and act accordingly. Since corrosion is a problem that is very hard to predict especially for new engineers and also a problem that is very resource consuming, i believe that the research done here and further research on this matter will contribute greatly in many different aspects. The model and methodology discussed in this paper are at their primal stages and there is much to be improved upon. I hope that the new approach on this matter, with the tools that technology has provided us with, can lead to new innovations on the field of civil engineering that all of us will take advantage of.

BIBLIOGRAPHY

Ababneh, A., Benboudjema, F., and Xi, Y. (2003). "Chloride Penetration in Nonsaturated Concrete." *Journal of Materials in Civil Engineering*, 15(2), 183–191.

"AL Technologies - Building Technology." (n.d.). <http://www.alt.com.sg/building_technology.html> (Dec. 14, 2014).

Bertolini, Luca, Elsener, Bernhard, Pedeferri, Pietro, Redaelli, Elena, Polder, R. (2013). *Corrosion of Steel in Concrete*.

"Carbonation of Concrete." (n.d.). <https://pavemaintenance.wikispaces.com/Carbonation+of+Concrete+-+Dahee> (Sep. 14, 2015).

Chen, M., Wang, K., Wu, Q., and Qin, Z. (2012). "An Experimental Corrosion Investigation of Coupling Chloride Ions with Stray Current for Reinforced Concrete." *Applied Mechanics and Materials*, 166-169(2012), 1987–1993.

Cheng, P. J. (2012). "The Accuracy Comparison of Assessing the Amount of Steel Corrosion in Concrete with Several Different Algorithms." *Applied Mechanics and Materials*, 166-169(2012), 1958–1962.

Frangopol, D., Lin, K.-Y., and Estes, A. (1997). "RELIABILITY OF REINFORCED CONCRETE GIRDERS UNDER CORROSION ATTACK." 286–297.

Hansen, E. J. D. P., Ekman, T., and Hansen, K. K. (2015). "Durability of Cracked Fibre Reinforced Concrete Structures Exposed to Chlorides." 8, 280–289.

Hussain, R. R., and Ishida, T. (2009). "Critical carbonation depth for initiation of steel corrosion in fully carbonated concrete and development of electrochemical carbonation induced corrosion model." *International Journal of Electrochemical Science*, 4(8), 1178–1195.

"Kamta Corporation - Goa , INDIA." (n.d.). <http://www.kamtacorporation.com/products/mc12.php> (Dec. 14, 2014).

Keun-Hyeok Yang, Eun-A Seo, S.-H. T. (2014). "Carbonation and CO2 uptake of concrete." *Environmental Impact Assessment Review*, 46, 43–52.

Kondratova, I., Montes, P., and Bremner, T. W. (2003). "Natural Marine Exposure Results for Reinforced Concrete Slabs with Corrosion Inhibitors."

Liu, R. G., Li, J., and Li, H. (2012). "Research on Chloride Diffusion Model in Pre-Stressed Concrete with Sulfate Attack." *Applied Mechanics and Materials*, 166-169(2012), 1935–1940.

El Maaddawy, T., and Soudki, K. (2007). “A model for prediction of time from corrosion initiation to corrosion cracking.” *Cement and Concrete Composites*, 29(3), 168–175.

“Map Analysis Topic 19: Routing and Optimal Paths.” (n.d.). <http://www.innovativegis.com/basis/mapanalysis/topic19/topic19.htm> (Sep. 14, 2015).

McCarter, W. J., and Vennesland, Ø. (2004). “Sensor systems for use in reinforced concrete structures.” *Construction and Building Materials*, 18(6), 351–358.

Millard, S. G., Law, D., Bungey, J. H., and Cairns, J. (2001). “Environmental in ¯ uences on linear polarisation corrosion rate measurement in reinforced concrete.” 34, 409–417.

Naik, B. T. R., and Science, A. (2004). “Utilization CARBONATION DEPTH TEST , AND.” (August).

NORDTEST. (1999). “CONCRETE, MORTAR AND CEMENT-BASED REPAIR MATERIALS: CHLORIDE MIGRATION COEFFICIENT FROM NON-STEADY-STATE MIGRATION EXPERIMENTS.” 1–8.

Ph. Turcry, L. Oksri-Nelfia, A. Younsi, A. A.-M. (2014). “Analysis of an accelerated carbonation test with severe preconditioning.” *Cement and Concrete Research*, 57, 70–78.

Pietro, P. (2013). *Fatigue and Corrosion in Metals*.

Pour-Ghaz, M., Isgor, O. B., and Ghods, P. (2009). “The effect of temperature on the corrosion of steel in concrete. Part 1: Simulated polarization resistance tests and model development.” *Corrosion Science*, Elsevier Ltd, 51(2), 415–425.

Raupach, M., and Gulikers, J. (2015). “A Simplified Method to Estimate Corrosion Rates A New Approach Based on Investigations of Macrocells.” 8, 376–385.

Saha, J. K. (2013). *Corrosion of Constructional Steels in Marine and Industrial Environment*. Springer.

SOHAIL, M. G. (2013). “Corrosion of Steel in Concrete: Development of an Accelerated Test by Carbonation and Galvanic Coupling.” Université Toulouse.

Song, H., and Saraswathy, V. (2007). “Corrosion Monitoring of Reinforced Concrete Structures - A Review.” *International Journal of Electrochemical Science*, 2, 1– 28.

Song, W. J., Dong, J., Bai, Y., Dong, F., and Sun, W. Z. (2012). “Investigation of Numerical Modeling for Concrete Corroded by Chloride Ion Diffusion.” *Applied Mechanics and Materials*, 166-169(2012), 1922–1925.

Thoft-Christensen, P. (2000). “Modelling of the Deterioration of Reinforced Concrete Structures.”

Zhu, X. E., and Dai, M. X. (2012). “A Discuss on Basing Half-Cell Potential Method for Estimating Steel Corrosion Rate in Concrete.” *Applied Mechanics and Materials*, 166-169(2012), 1926–1930.

ANNEXES

QGIS Attributes Table

id	P	S	rm	rt	D	i	E	f	C	Psi	N1	N2	Risk
1	0,07	0,10	0,10	0,06	8,00	16,00	22,00	3,00	20,00	0,057143	3,40988	3,16584	130,33907
2	0,10	0,90	0,01	0,00	15,00	762,00	27,00	5,00	40,00	0,051136	0,51148	0,17065	165,72333
3	0,15	0,13	0,02	0,01	21,00	287,00	23,00	3,00	50,00	0,062113	6,94169	0,40355	195,59416
4	0,03	0,24	0,00	0,00	9,00	345,00	26,00	4,00	30,00	0,034615	0,22953	0,23131	127,20459
5	0,05	0,98	7,00	4,20	29,00	42,00	25,00	3,00	22,00	0,374777	0,05436	4,43527	52,85250
6	0,17	0,76	0,00	0,00	14,00	98,00	30,00	3,00	25,00	0,100513	0,89920	0,46507	151,84359
7	0,08	0,25	0,04	0,02	30,00	671,00	22,00	6,00	21,00	0,420168	3,22631	0,19579	195,24632
8	0,04	0,46	0,00	0,00	22,00	902,00	31,00	4,00	70,00	0,037578	0,21745	0,17356	136,08729
9	0,20	0,39	0,04	0,02	16,00	387,00	33,00	3,00	30,00	0,092754	6,56016	0,12979	201,03171
10	0,23	0,01	0,50	0,30	18,00	63,00	23,00	7,00	40,00	0,069828	12,36763	3,74190	168,46134
11	0,21	0,08	0,40	0,24	11,00	287,00	30,00	5,00	20,00	0,097581	0,10491	0,24643	200,48878
12	0,12	0,84	0,60	0,36	15,00	911,00	24,00	3,00	45,00	0,041667	1,04301	0,12534	187,58584
13	0,12	0,54	0,00	0,00	9,00	781,00	26,00	4,00	60,00	0,009783	2,08392	0,20024	190,58742
14	0,11	0,36	0,01	0,00	7,00	276,00	29,00	5,00	22,00	0,038401	3,51762	0,23896	194,26758
15	0,07	0,22	0,10	0,06	6,00	451,00	28,00	6,00	23,00	0,026987	2,95523	0,19718	194,43021
16	0,15	0,05	0,02	0,01	27,00	761,00	22,00	3,00	45,00	0,112500	7,58000	0,14895	201,05137
17	0,18	0,68	0,08	0,05	21,00	483,00	27,00	5,00	20,00	0,268902	3,11420	0,16172	196,44700
18	0,03	0,32	0,00	0,00	14,00	917,00	31,00	3,00	70,00	0,016667	0,58990	0,12586	177,09685
19	0,03	0,29	0,00	0,00	12,00	734,00	22,00	3,00	21,00	0,103896	0,71101	0,07133	190,05114
20	0,08	0,58	0,00	0,00	16,00	548,00	30,00	4,00	22,00	0,153110	1,26848	0,10162	192,65222
21	0,06	0,26	0,00	0,00	8,00	69,00	33,00	4,00	30,00	0,028070	1,48211	0,90659	145,93141

22	0,17	0,18	0,01	0,00	29,00	259,00	26,00	6,00	21,00	0,400476	7,06047	0,42147	195,38134
23	0,19	0,04	0,70	0,42	20,00	94,00	28,00	3,00	45,00	0,068376	9,90963	10,81297	188,94772
24	0,23	0,92	0,00	0,00	23,00	568,00	32,00	7,00	50,00	0,072466	0,90743	0,34355	161,98232
25	0,21	0,81	0,00	0,00	7,00	826,00	22,00	3,00	60,00	0,006095	1,29350	0,16728	186,47885
26	0,05	0,70	0,07	0,04	18,00	46,00	29,00	3,00	20,00	0,213158	0,81036	0,92058	122,62871
27	0,15	0,72	0,05	0,03	12,00	29,00	23,00	4,00	30,00	0,057143	2,26294	32,18274	114,16658
28	0,14	0,61	5,00	3,00	14,00	749,00	33,00	7,00	65,00	0,019085	2,96797	0,63368	177,08110
29	0,20	0,50	0,30	0,18	6,00	265,00	24,00	3,00	21,00	0,031746	5,42836	0,20407	198,45672
30	0,09	0,02	0,00	0,00	30,00	536,00	32,00	7,00	45,00	0,133333	2,76625	0,34337	187,10536
31	0,14	0,91	0,00	0,00	27,00	63,00	25,00	5,00	40,00	0,136007	0,39518	2,37908	72,79406
32	0,12	0,14	0,07	0,04	21,00	487,00	30,00	4,00	55,00	0,052751	5,57369	0,26789	196,98357
33	0,04	0,30	0,00	0,00	15,00	632,00	22,00	3,00	21,00	0,148810	0,47568	0,08571	180,63963
34	0,22	0,09	0,00	0,00	13,00	523,00	33,00	7,00	22,00	0,109740	7,02163	0,16386	200,51092
35	0,21	0,20	0,00	0,00	19,00	83,00	31,00	6,00	25,00	0,164091	6,94904	1,11582	182,83153
36	0,18	0,41	0,00	0,00	22,00	631,00	23,00	6,00	20,00	0,288095	1,06914	0,17280	182,71206
37	0,17	0,49	0,03	0,02	25,00	505,00	32,00	3,00	30,00	0,189394	4,64517	0,10967	200,47105
38	0,11	0,51	0,01	0,00	30,00	304,00	28,00	7,00	23,00	0,369155	2,69318	0,41748	183,46598
39	0,09	0,11	0,30	0,18	7,00	284,00	27,00	3,00	65,00	0,005235	4,34812	0,48087	188,76429
40	0,20	0,56	0,01	0,00	9,00	381,00	32,00	5,00	60,00	0,009783	4,39703	0,41740	190,73537
41	0,04	0,03	0,01	0,00	10,00	367,00	22,00	3,00	55,00	0,013986	1,96518	0,34799	180,98307
42	0,12	0,80	0,00	0,00	22,00	581,00	32,00	4,00	20,00	0,288095	0,87630	0,08995	189,75651
43	0,11	0,19	0,00	0,00	12,00	835,00	25,00	3,00	55,00	0,019539	2,30656	0,13498	195,54122
44	0,17	0,23	0,71	0,43	15,00	946,00	26,00	3,00	65,00	0,021635	0,71117	0,15913	200,65136
45	0,15	0,06	0,80	0,48	24,00	734,00	22,00	4,00	21,00	0,304762	0,76610	0,13279	201,39321
46	0,19	0,99	0,00	0,00	28,00	543,00	30,00	7,00	55,00	0,085871	0,06937	0,42593	72,42973
47	0,20	0,94	0,00	0,00	21,00	238,00	29,00	6,00	50,00	0,062113	0,56892	0,76894	116,06274
48	0,22	0,21	0,07	0,04	13,00	538,00	22,00	3,00	45,00	0,032375	9,38932	0,20082	200,79619
49	0,08	0,31	0,01	0,00	7,00	741,00	33,00	7,00	55,00	0,007185	2,75814	0,26655	190,51684
50	0,07	0,07	0,04	0,02	11,00	385,00	23,00	5,00	20,00	0,097581	3,50054	0,20835	195,40502
51	0,13	0,16	0,01	0,01	29,00	356,00	32,00	3,00	70,00	0,060678	5,65977	0,32613	195,66420

52	0,03	0,69	0,01	0,01	26,00	484,00	27,00	4,00	21,00	0,342452	0,48427	0,13971	169,74354
53	0,06	0,62	0,00	0,00	16,00	85,00	31,00	3,00	23,00	0,142698	0,59023	0,49314	134,35605
54	0,15	0,15	0,20	0,12	22,00	267,00	30,00	3,00	40,00	0,097581	6,91610	0,28807	197,88203
55	0,21	0,65	1,00	0,60	12,00	681,00	24,00	4,00	50,00	0,023226	3,99394	0,26543	194,46561
56	0,18	0,12	0,00	0,00	14,00	673,00	25,00	3,00	21,00	0,133333		0,07000	0,00000
57	0,13	0,28	0,50	0,30	11,00	852,00	29,00	3,00	30,00	0,049187	5,08393	0,07788	201,69148
58	0,11	0,88	0,01	0,00	10,00	634,00	26,00	7,00	20,00	0,083333	0,68018	0,15316	175,88024
59	0,18	0,82	0,90	0,54	6,00	931,00	22,00	3,00	20,00	0,034615	1,76051	0,07961	197,38105
60	0,05	0,17	0,03	0,02	8,00	532,00	22,00	3,00	55,00	0,009235	2,22346	0,24125	189,02413
61	0,09	0,60	0,00	0,00	8,00	34,00	33,00	4,00	22,00	0,048485	1,76313	1,37461	136,97232
62	0,10	0,77	0,00	0,00	14,00	934,00	23,00	7,00	23,00	0,115159	0,50690	0,13819	171,22537
63	0,10	0,79	0,00	0,00	16,00	475,00	29,00	5,00	60,00	0,028070	0,54363	0,37455	141,58698
64	0,12	0,86	0,00	0,00	18,00	854,00	32,00	7,00	21,00	0,197802	0,74861	0,10556	185,09239
65	0,23	0,89	0,08	0,05	6,00	134,00	22,00	5,00	25,00	0,023226	1,36787	0,75412	149,62641
66	0,11	0,27	0,00	0,00	20,00	273,00	32,00	7,00	55,00	0,048485	2,51848	0,77076	168,14790
67	0,16	0,55	0,00	0,00	14,00	632,00	22,00	3,00	20,00	0,144118	1,58682	0,08135	196,53892
68	0,05	0,43	0,01	0,00	8,00	475,00	28,00	4,00	55,00	0,009235	1,42404	0,28052	178,82036
69	0,03	0,83	0,10	0,06	12,00	634,00	33,00	6,00	40,00	0,034615	0,27604	0,20389	139,00066
70	0,17	0,96	0,00	0,00	14,00	236,00	32,00	7,00	60,00	0,022072	0,06846	0,95167	61,26738
71	0,21	0,53	0,10	0,06	8,00	734,00	23,00	7,00	50,00	0,011034	5,34215	0,36223	194,28451
72	0,22	0,67	0,00	0,00	8,00	237,00	25,00	3,00	70,00	0,005861	0,40273	0,59831	112,55355
73	0,23	0,35	0,00	0,00	20,00	731,00	27,00	4,00	20,00	0,250000	4,68883	0,08253	201,35370
74	0,14	0,45	0,01	0,00	24,00	175,00	30,00	6,00	55,00	0,066283	3,84740	1,11601	169,59835
75	0,18	0,87	0,07	0,04	20,00	235,00	32,00	3,00	21,00	0,232288	1,26415	0,17384	185,50346
76	0,12	0,44	0,01	0,01	18,00	23,00	31,00	3,00	45,00	0,057143	0,34992	3,34432	129,23176
77	0,20	0,47	0,01	0,00	16,00	732,00	23,00	5,00	55,00	0,032778	5,36879	0,28232	196,35644
78	0,19	0,85	0,00	0,00	12,00	47,00	29,00	7,00	20,00	0,112500	0,15810	1,88986	62,81124
79	0,06	0,93	10,00	6,00	8,00	632,00	24,00	3,00	50,00	0,011034	0,22832	0,81207	84,57636
80	0,03	0,38	0,01	0,01	10,00	356,00	25,00	4,00	30,00	0,041667	0,96854	0,23535	174,09022
81	0,12	0,42	0,50	0,30	6,00	76,00	28,00	6,00	22,00	0,029221	3,78036	1,33935	163,97421

82	0,08	0,33	0,00	0,00	16,00	634,00	27,00	4,00	60,00	0,028070	2,38842	0,24121	189,96559
83	0,21	0,97	0,40	0,24	26,00	845,00	26,00	5,00	40,00	0,128030	0,34211	0,18146	150,97391
84	0,23	1,00	0,07	0,04	22,00	532,00	32,00	4,00	70,00	0,037578	0,00000	0,28876	0,00000
85	0,20	0,37	0,00	0,00	18,00	743,00	33,00	5,00	20,00	0,213158	0,36827	0,08088	176,44763
86	0,15	0,34	2,00	1,20	16,00	262,00	22,00	7,00	45,00	0,046630	5,38078	1,30146	174,20102
87	0,16	0,48	0,00	0,00	22,00	17,00	22,00	3,00	20,00	0,288095	0,83760	3,35279	81,58247
88	0,19	0,52	0,00	0,00	28,00	332,00	22,00	3,00	50,00	0,100513	4,32378	0,37455	191,80275
89	0,10	0,95	0,50	0,30	8,00	532,00	26,00	5,00	21,00	0,052545	0,27158	0,16322	146,56590
90	0,13	0,57	0,01	0,01	10,00	125,00	30,00	4,00	23,00	0,065876	2,89726	0,43691	183,95096
91	0,05	0,40	0,00	0,00	12,00	37,00	25,00	7,00	25,00	0,077838	0,08768	3,38751	54,86034
92	0,11	0,59	0,00	0,00	12,00	856,00	28,00	3,00	55,00	0,019539	1,30414	0,11757	191,34764
93	0,06	0,66	0,01	0,01	20,00	672,00	29,00	6,00	22,00	0,216450	1,06227	0,13499	186,74925
94	0,07	0,64	9,00	5,40	18,00	732,00	31,00	4,00	60,00	0,034615	1,36989	0,54075	160,69760
95	0,20	0,71	1,00	0,60	26,00	834,00	27,00	4,00	30,00	0,201190	3,15168	0,12990	197,94337
96	0,22	0,63	0,00	0,00	10,00	436,00	23,00	6,00	20,00	0,083333	0,45155	0,21520	154,61714
97	0,13	0,78	0,01	0,00	8,00	732,00	25,00	3,00	40,00	0,016667	1,44856	0,11199	193,02059
98	0,18	0,74	0,00	0,00	6,00	234,00	26,00	5,00	70,00	0,003383	1,70879	0,96943	148,61891
99	0,16	0,75	0,60	0,36	14,00	71,00	28,00	3,00	23,00	0,115159	2,17294	0,81505	162,26548
100	0,07	0,73	0,00	0,00	16,00	543,00	24,00	4,00	50,00	0,038788	0,89605	0,26644	168,93286

Corrosion Risk Map